Finite-dimensional approximation and control of non-linear parabolic PDE systems

JAMES BAKER† and PANAGIOTIS D. CHRISTOFIDES†‡

This article proposes a rigorous and practical methodology for the derivation of accurate finite-dimensional approximations and the synthesis of non-linear output feedback controllers for non-linear parabolic PDE systems for which the manipulated inputs, the controlled and measured outputs are distributed in space. The method consists of three steps: first, the Karhunen–Loéve expansion is used to derive empirical eigenfunctions of the non-linear parabolic PDE system, then the empirical eigenfunctions are used as basis functions within a Galerkin's and approximate inertial manifold model reduction framework to derive low-order ODE systems that accurately describe the dominant dynamics of the PDE system, and finally, these ODE systems are used for the synthesis of non-linear output feedback controllers that guarantee stability and enforce output tracking in the closed-loop system. The proposed method is used to perform model reduction and synthesize a non-linear dynamic output feedback controller for a rapid thermal chemical vapour deposition process. The controller uses measurements of wafer temperature at five locations to manipulate the power of the top lamps in order to achieve spatially uniform temperature, and thus, uniform deposition of the thin film on the wafer over the entire process cycle. The performance of the non-linear controller is successfully tested through simulations and is shown to be superior to the one of a linear controller.

1. Introduction

There are many industrially important diffusion–convection–reaction processes which are naturally described by non-linear parabolic partial differential equation (PDE) systems. Examples include rapid thermal processing, plasma reactors, crystal growth processes to name a few. The main feature of parabolic PDEs is that their dominant dynamic behaviour is usually characterized by a finite (typically small) number of degrees of freedom (Temam 1988) (for example, in the case of systems with linear spatial differential operators this follows from the fact that the eigenspectrum of the spatial differential operator can be partitioned into a finite-dimensional slow one and an infinite-dimensional stable fast complement). This implies that the dynamic behaviour of such systems can be *approximately* described by ordinary differential equation (ODE) systems. Therefore, the standard approach to the control of quasi-linear parabolic PDE systems (i.e. systems which include linear spatial differential operators and non-linear terms that enter the system in an additive fashion) involves the application of Galerkin's method (where the basis used to expand the solution of the system are typically the eigenfunctions of the spatial differential operator) to the PDE system to derive ODE systems that accurately describe the dynamics of the dominant (slow) modes of the PDE system, which are subsequently used as the basis for controller synthesis (see, for example, Balas 1979, Ray 1981, Chen and Chang 1992). The main disadvantage of this

approach is that the number of modes that should be retained to derive an ODE system that yields the desired degree of approximation may be very large, leading to complex controller design and high dimensionality of the resulting controllers.

A natural approach to the construction of low-dimensional ODE systems that accurately reproduce the dynamics and solutions of quasi-linear parabolic PDE systems is based on the concept of inertial manifold (IM) (see, for example, Temam 1988 and references therein). An IM is a finite-dimensional Lipschitz manifold which is positively invariant and attracts every trajectory of the system exponentially. When the trajectories of the parabolic PDE system are on the IM, it is *exactly* described by a dynamical system (called inertial form) whose dimension is equal to the number of slow modes. However, the explicit derivation of the inertial form requires the computation of the closed-form expression of the IM, which is a very difficult task in most practical applications. In order to overcome this problem, a novel procedure, based on singular perturbations, was proposed in Christofides and Daoutidis (1997) for the construction of approximations of the inertial manifold (called approximate inertial manifolds (AIMs)), which were used to derive ODE systems of dimension equal to the number of slow modes, that yield solutions which are close, up to a desired accuracy, to the ones of the PDE system (see also Foias *et al.* 1989 for alternative approaches for the construction of AIMs). These ODE systems were used as the basis for the synthesis of non-linear output feedback controllers that guarantee stability and enforce the output of the closed-loop system to follow, up to a desired accuracy, a prespecified response. These results were extended in Christofides (1998) to quasi-linear parabolic PDE

systems with uncertainty, leading to the design of robust non-linear controllers. The reader may refer to the recent book by Christofides (2000) for detailed results and references in this area.

Unfortunately, the developed control methods for quasi-linear parabolic PDE systems cannot be directly employed for the design of low-dimensional controllers for systems that include non-linear spatial differential operators. The reason is that the eigenvalue problems of non-linear spatial differential operators cannot be, in general, solved analytically, and thus, it is difficult to *a priori* (without having any information about the solution of the system) choose an optimal (in the sense that will lead to a low-dimensional ODE system) basis to expand the solution of the PDE system. An approximate way to address this problem (Ray 1981) is to linearize the non-linear spatial differential operator around a steady state and address the controller design problem on the basis of the resulting quasi-linear system. However, this approach is only valid in a small neighbourhood of the steady state where the linearization is valid. An alternative approach which is not based on linearization is to utilize detailed finite difference (element) simulations of the PDE system to compute a set of empirical eigenfunctions (dominant spatial patterns) of the system through Karhunen–Loéve expansion (also known as proper orthogonal decomposition and principal component analysis). The use of empirical eigenfunctions as basis functions in Galerkin's method has been shown to lead to the derivation of accurate non-linear low-dimensional approximations of several dissipative PDE systems arising in the modelling of diffusion–reaction processes and fluid flows (Park and Cho 1996, Bangia *et al.* 1997, Banerjee *et al.* 1998, Theodoropoulou *et al.* 1998). Recently, linear feedback controllers were synthesized in Shvartsman and Kevrekidis (1998) and Theodoropou-lou *et al.* (1999) for specific diffusion-reaction systems on the basis of low-dimensional models obtained by using empirical eigenfunctions as basis functions in Galerkin's method. At this stage, a rigorous method for the design of non-linear output feedback controllers for general non-linear parabolic PDE systems on the basis of ODE models which are constructed by combining Galerkin's method with empirical eigenfunctions is not available.

In this paper, we consider non-linear parabolic PDE systems for which the manipulated inputs, the controlled and measured outputs are distributed in space, and propose a general method for the derivation of finite-dimensional approximation and the synthesis of non-linear output feedback controllers. The method is applied to a rapid thermal chemical vapour deposition (RTCVD) process.

The paper is structured as follows: Initially, the class of non-linear parabolic PDE systems considered in this work is given and the key steps of the proposed model reduction and control method are articulated. Then, the method is presented in detail: first, the Karhunen–Loéve expansion is used to derive empirical eigenfunctions of the non-linear parabolic PDE system, then the empirical eigenfunctions are used as basis functions within a Galerkin's and approximate inertial manifold model reduction framework to derive low-order ODE systems that accurately describe the dominant dynamics of the PDE system, and finally, these ODE systems are used for the synthesis of non-linear dynamic output feedback controllers that guarantee stability and enforce output tracking in the closed-loop system. Finally, an application of the proposed method to non-linear model reduction and control of an RTCVD process is presented. The performance of the non-linear controller is successfully tested through simulations and is shown to be superior to the one of a linear controller.

2. Nonlinear parabolic PDE systems

2.1. *Description of class of systems*

We consider non-linear parabolic PDE systems in one spatial dimension with the following state space description

$$\left. \begin{array}{l} \dfrac{\partial \bar{x}}{\partial t} = L(\bar{x}) + wb(z)u + f(\bar{x}) \\[2mm] y^i = \displaystyle\int_\alpha^\beta c^i(z)k\bar{x}\,\mathrm{d}z, \qquad i = 1,\ldots,l \end{array} \right\} \quad (1)$$

subject to the boundary conditions

$$\left. \begin{array}{l} C_1\bar{x}(\alpha,t) + D_1\dfrac{\partial \bar{x}}{\partial z}(\alpha,t) = R_1 \\[2mm] C_2\bar{x}(\beta,t) + D_2\dfrac{\partial \bar{x}}{\partial z}(\beta,t) = R_2 \end{array} \right\} \quad (2)$$

and the initial condition

$$\bar{x}(z,0) = \bar{x}_0(z) \quad (3)$$

where $\bar{x}(z,t) = [\bar{x}_1(z,t) \;\cdots\; \bar{x}_n(z,t)]^{\mathrm{T}}$ denotes the vector of state variables, $z \in [\alpha,\beta] \subset \mathbb{R}$ is the spatial coordinate, $t \in [0,\infty)$ is the time, $u = [u^1\, u^2\, \cdots\, u^l]^{\mathrm{T}} \in \mathbb{R}^l$ denotes the vector of manipulated inputs, and $y^i \in \mathbb{R}$ denotes the ith controlled output. $L(\bar{x})$ is a non-linear differential operator which involves first- and second-order spatial derivatives, $f(\bar{x})$ is a non-linear vector function, w,k are constant vectors, A,B,C_1,D_1,C_2,D_2 are constant matrices, R_1,R_2 are column vectors, and $\bar{x}_0(z)$ is the initial condition. $b(z)$ is a known smooth vector function of z of the form $b(z) = [b^1(z)\, b^2(z)\, \cdots\, b^l(z)]$, where $b^i(z)$ describes how the control action $u^i(t)$ is distributed in the interval $[\alpha,\beta]$, and $c^i(z)$ is a known smooth function of z which is determined by the desired performance specifications

in the interval $[\alpha, \beta]$. Whenever the control action enters the system at a single point z_0, with $z_0 \in [\alpha, \beta]$ (i.e. point actuation), the function $b^i(z)$ is taken to be non-zero in a finite spatial interval of the form $[z_0 - \epsilon, z_0 + \epsilon]$, where ϵ is a small positive real number, and zero elsewhere in $[\alpha, \beta]$. Throughout the paper, we will use the order of magnitude notation $O(\epsilon)$. In particular, $\delta(\epsilon) = O(\epsilon)$ if there exist positive real numbers k_1 and k_2 such that: $|\delta(\epsilon)| \le k_1 |\epsilon|, \ \forall \ |\epsilon| < k_2$. Furthermore, $L_f h$ denotes the standard Lie derivative of a scalar field h with respect to the vector field f, $L_f^k h$ denotes the k-th order Lie derivative and $L_g L_f^{k-1} h$ denotes the mixed Lie derivative. Finally, in order to simplify the presentation of the theoretical results, we will not consider measured outputs separately from the controlled outputs, which means that we need to assume the availability of on-line measurements of the controlled outputs, $y^i(t)$.

In order to simplify the presentation of the theoretical results of the paper, we formulate the parabolic PDE system of equation (1) in an infinite dimensional system in the Hilbert space $\mathcal{H}([\alpha, \beta], \mathbb{R}^n)$ (this allows us to incorporate directly the boundary conditions of equation (2) in the formulation; see equation (5) below), with $\mathcal{H}$ being the space of n-dimensional vector functions defined on $[\alpha, \beta]$ that satisfy the boundary condition of equation (2), with inner product and norm

$$(\omega_1, \omega_2) = \int_\alpha^\beta (\omega_1(z), \omega_2(z))_{\mathbb{R}^n} \, \mathrm{d}z$$

$||\omega_1||_2 = (\omega_1, \omega_1)^{1/2}$ where ω_1, ω_2 are two elements of $\mathcal{H}([\alpha, \beta]; \mathbb{R}^n)$ and the notation $(\cdot, \cdot)_{\mathbb{R}^n}$ denotes the standard inner product in $\mathbb{R}^n$. Defining the state function x on $\mathcal{H}([\alpha, \beta], \mathbb{R}^n)$ as $x(t) = \bar{x}(z, t), \ t > 0, \ z \in [\alpha, \beta]$, the operator $\mathcal{A}$ in $\mathcal{H}([\alpha, \beta], \mathbb{R}^n)$ as

$$\mathcal{A}(x) = L(\bar{x})$$

$$x \in D(\mathcal{A}) = \left\{ \begin{array}{c} x \in \mathcal{H}([\alpha, \beta]; \mathbb{R}^n) \\ C_1 \bar{x}(\alpha, t) + D_1 \dfrac{\partial \bar{x}}{\partial z}(\alpha, t) = R_1 \\ C_2 \bar{x}(\beta, t) + D_2 \dfrac{\partial \bar{x}}{\partial z}(\beta, t) = R_2 \end{array} \right\} \quad (4)$$

and the input and output operators as $\mathcal{B}u = wbu$, $\mathcal{C}x = (c, kx)$, where $c = [c^1 \ c^2 \ \cdots c^l]$, the system of equations (1)–(2) takes the form

$$\left. \begin{array}{l} \dot{x} = \mathcal{A}(x) + \mathcal{B}u + f(x), \qquad x(0) = x_0 \\ y = \mathcal{C}x \end{array} \right\} \quad (5)$$

where $f(x(t)) = f(\bar{x}(z, t))$ and $x_0 = \bar{x}_0(z)$. We assume that the non-linear terms $f(x)$ are locally Lipschitz with respect to their arguments and satisfy $f(0) = 0$. Finally, motivated by our objective to develop model reduction and control methods for non-linear parabolic

PDEs that describe transport-reaction processes of practical interest, we will assume throughout the paper that the system of equation (1) (with and without feedback control) has a unique solution which is also sufficiently smooth (i.e. all the spatial and time derivatives in the system of equation (1) are smooth functions of space and time).

2.2. *Methodology for model reduction and control*

The main obstacles in developing a general model reduction and control method for systems of the form of equation (1) are: (a) the spatial differential operator is non-linear, and (b) the domain of definition of the process is generally irregular (e.g. a chemical reactor with complex geometry). These issues do not allow the computation of analytic expressions for the eigenvalues and eigenfunctions of the system, and thus, they prohibit the direct use of Galerkin's methods or orthogonal collocation methods with standard basis function sets, to derive finite dimensional approximations of the PDE system.

To overcome the above problems, we employ the following methodology for the derivation of finite-dimensional approximations and the synthesis of low-dimensional non-linear output feedback controllers for systems of the form of equation (1).

(1) Initially, assuming that the solution of the parabolic PDE system of equation (1) is known, a set of empirical eigenfunctions (dominant spatial patterns) of the system will be computed using Karhunen–Loéve expansion.

(2) These empirical eigenfunctions will be then used as basis functions within a Galerkin's and approximate inertial manifold model reduction framework to derive low-dimensional ODE systems that accurately reproduce the solutions of the non-linear PDE system.

(3) These ODE systems are used as a basis for the synthesis of low dimensional non-linear controllers, which use on-line measurements of process outputs to stabilize the closed-loop system and force the output to follow the set-point. Finally, it is established that the output of the infinite-dimensional closed-loop system (PDE model and controller) satisfies $y_i(t) = y_s^i(t) + O(\bar{\epsilon}), \ t \ge 0$, where $y_s^i(t)$ being the ith output of the closed-loop slow subsystem and $\bar{\epsilon}$ is a small positive parameter which depends on the degree of approximation of the original parabolic PDE model from the finite-dimensional system.

Remark 1: We note that the above control methodology can be readily generalized to systems of coupled

non-linear parabolic PDEs and non-linear ordinary differential equations of the form:

$$\left.\begin{array}{l} \dfrac{\partial \hat{x}}{\partial t} = \hat{f}(\bar{x},\hat{x},u) \\[2mm] \dfrac{\partial \bar{x}}{\partial t} = L(\bar{x}) + wb(z)u + f(\bar{x},\hat{x}) \\[2mm] y^i = \displaystyle\int_\alpha^\beta c^i(z)k\bar{x}dz, \qquad i=1,\dots,l \end{array}\right\} \quad (6)$$

3. Computation of empirical eigenfunctions via Karhunen–Loéve expansion

In this section, we review the K–L expansion in the context of non-linear one-dimensional parabolic PDE systems of the form of equation (1) with $n=1$ (see Fukunaga 1990, Holmes *et al.* 1996 for a general presentation and analysis of the K–L expansion). We assume that the solution of the system of equation (1) is known and consider a sufficiently large set (ensemble), $\{\bar{v}_\kappa\}$, consisting of N sampled states, $\bar{v}_\kappa(z)$ (which are typically called 'snapshots'), of the solution of equation (1). To simplify our presentation, we assume uniform in time sampling of, $\bar{v}_\kappa(z)$ (i.e. the time interval between any two successive sampled states is the same), while we define the ensemble average of snapshots as $\langle \bar{v}_\kappa \rangle := 1/K\sum_{n=1}^{K} \bar{v}_n(z)$ (we note that non-uniform sampling of the snapshots and weighted ensemble average can be also considered; see, for example, Graham and Kevrekidis (1996)). Furthermore, the ensemble average of snapshots $\langle \bar{v}_\kappa \rangle$ is subtracted out from the snapshots, i.e.

$$v_\kappa = \bar{v}_\kappa - \langle \bar{v}_\kappa \rangle \qquad (7)$$

so that only fluctuations are analysed. The issue is how to obtain the most typical or characteristic structure $\phi(z)$ among these snapshots $\{v_\kappa\}$. Mathematically, this problem can be posed as the one of obtaining a function $\phi(z)$ that maximizes the objective function

$$\text{Maximize } \frac{\langle (\phi,v_\kappa)^2 \rangle}{(\phi,\phi)} \quad \text{s.t. } (\phi,\phi)=1, \quad \phi \in L^2([\alpha,\beta]) \qquad (8)$$

The constraint $(\phi,\phi)=1$ is imposed to ensure that the function, $\phi(z)$, computed as a solution of the above maximization problem, is unique. The Lagrangian functional corresponding to this constrained optimization problem is

$$\bar{L} = \langle (\phi,v_\kappa)^2 \rangle - \lambda((\phi,\phi)-1) \qquad (9)$$

and necessary conditions for extrema is that the functional derivative vanishes for all variations $\phi + \delta\psi \in L^2[\alpha,\beta]$, where δ is a real number:

$$\frac{d\bar{L}(\phi+\delta\psi)}{d\delta}(\delta=0)=0, \qquad (\phi,\phi)=1 \qquad (10)$$

Using the definitions of inner product and ensemble average, $d\bar{L}(\phi+\delta\psi)/d\delta\ (\delta=0)$ can be computed as

$$\begin{aligned} \frac{d\bar{L}(\phi+\delta\psi)}{d\delta}(\delta=0) &= \frac{d}{d\delta}[\langle (v_\kappa,\phi+\delta\psi)(\phi+\delta\psi,v_\kappa)\rangle \\ &\quad - \lambda(\phi+\delta\psi,\phi+\delta\psi)]_{\delta=0} \\ &= 2\mathrm{Re}[\langle (v_\kappa,\psi)(\phi,v_\kappa)\rangle - \lambda(\phi,\psi)] \\ &= \left\langle \int_\alpha^\beta \psi(z)v_\kappa(z)\,dz \int_\alpha^\beta \phi(z)v_\kappa(z)\,dz \right\rangle \\ &\quad - \lambda \int_\alpha^\beta \phi(\bar{z})\psi(\bar{z})d\bar{z} \\ &= \int_\alpha^\beta \left(\left\{\int_\alpha^\beta \langle v_\kappa(z)v_\kappa(\bar{z})\rangle \phi(z)\,dz\right\} \right. \\ &\quad \left. - \lambda\phi(\bar{z})\right)\psi(\bar{z})\,d\bar{z} \end{aligned} \qquad (11)$$

Since $\psi(\bar{z})$ is an arbitrary function, the necessary conditions for optimality take the form

$$\int_\alpha^\beta \langle v_\kappa(z)v_\kappa(\bar{z})\rangle \phi(z)\,dz = \lambda\phi(\bar{z}), \qquad (\phi,\phi)=1 \qquad (12)$$

Introducing the two-point correlation function

$$K(z,\bar{z}) = \langle v_\kappa(z)v_\kappa(\bar{z})\rangle = \frac{1}{K}\sum_{\kappa=1}^{K} v_\kappa(z)v_\kappa(\bar{z}) \qquad (13)$$

and the linear operator

$$R := \int_\alpha^\beta K(z,\bar{z})\,d\bar{z} \qquad (14)$$

the optimality condition of equation (12) reduces to the eigenvalue problem of the integral equation:

$$R\phi = \lambda\phi \quad \Longrightarrow \quad \int_\alpha^\beta K(z,\bar{z})\phi(\bar{z})\,d\bar{z} = \lambda\phi(z) \qquad (15)$$

The computation of the solution of the above integral eigenvalue problem is, in general, a very expensive computational task. To circumvent this problem, Sirovich introduced in 1987 (Sirovich 1987a, b) the method of snapshots. The central idea of this technique is to assume that the requisite eigenfunction, $\phi(z)$, can be expressed as a linear combination of the snapshots, i.e.

$$\phi(z) = \sum_k c_k v_k(z) \qquad (16)$$

Substituting the above expression for $\phi(z)$ on equation (15), we obtain the eigenvalue problem

$$\int_\alpha^\beta \frac{1}{K}\sum_{\kappa=1}^{K} v_\kappa(z)v_\kappa(\bar{z}) \sum_{k=1}^{K} c_k v_k(\bar{z})\,d\bar{z} = \lambda \sum_{k=1}^{K} c_k v_k(z) \qquad (17)$$

Defining

$$B^{\kappa k} := \frac{1}{K} \int_\alpha^\beta v_\kappa(\bar{z}) v_k(\bar{z}) \, \mathrm{d}\bar{z} \qquad (18)$$

the eigenvalue problem of equation (17) can be equivalently written as

$$Bc = \lambda c \qquad (19)$$

The solution of the above eigenvalue problem (which can be obtained by utilizing standard methods from matrix theory) yields the eigenvectors $c = [c_1 \; \cdots \; c_K]$ which can be used in equation (16) to construct the eigenfunction $\phi(z)$. From the structure of the matrix B, it follows that it is symmetric and positive semi-definite, and thus, its eigenvalues, λ_κ, $\kappa = 1, \ldots, K$, are real and non-negative. Furthermore

$$\int_\alpha^\beta \phi_\kappa(z) \phi_k(z) \, \mathrm{d}z = 0, \qquad \kappa \neq k \qquad (20)$$

Remark 2: The optimality of the empirical eigenfunctions obtained via K–L expansion can be understood as follows. Consider a snapshot $v_\kappa(z)$ of the ensemble of snapshots, v_κ, and the set of empirical eigenfunctions obtained by applying K–L expansion to v_κ, and let

$$v_\kappa(z) = \sum_{l=1}^L \gamma_l \phi_l(z) \qquad (21)$$

be the decomposition of $v_\kappa(z)$ with respect to this basis. Assume that the eigenfunctions have been ordered so the corresponding eigenvalues satisfy $\lambda_1 > \lambda_2 > \cdots > \lambda_{l+1}$. Then, it can be shown (Holmes *et al.* 1996) that if $\{\psi_1, \psi_2, \ldots, \psi_\kappa\}$ is some arbitrary set of orthonormal basis functions in which we expand $v_\kappa(z)$, then the following result holds for any L

$$\sum_{l=1}^L \langle (\phi_l, v_\kappa)^2 \rangle = \sum_{l=1}^L \lambda_l \geq \sum_{l=1}^L \langle (\psi_l, v_\kappa)^2 \rangle \qquad (22)$$

This implies that the projection on the subspace spanned by the empirical eigenfunctions will on average contain the most energy possible compared to all other linear decompositions, for any number of modes L.

4. Derivation of finite-dimensional approximations

In this section, we use a combination of Galerkin's method with the concept of approximate inertial manifolds, known as *non-linear Galerkin's method*, to derive low-dimensional dynamical systems of non-linear ordinary differential equations that accurately reproduce the dynamics and solutions of the non-linear parabolic PDE system of equation (1). To this end, we assume that we have available an orthogonal and complete set of global

(in the sense that they span the entire domain of definition of the process) basis functions, $\phi_n(z)$, that satisfy the boundary conditions of equation (2). In practice, $\phi_n(z)$ may be the set of empirical eigenfunctions obtained through K–L expansion. In the remainder of this section, we precisely characterize the accuracy of the finite-dimensional approximations obtained through linear and non-linear Galerkin's method.

4.1. *Linear Galerkin's method*

Let $\mathcal{H}_a$ be a subspace, defined as

$$\mathcal{H}_a = \mathrm{span} \{\phi_1, \phi_2, , \phi_N\}$$

where ϕ_n $(n = 1, \ldots, N)$ denotes a basis function, and define P_a to be a projection operator from $\mathcal{H}([\alpha, \beta], \mathbb{R}^n)$ to $\mathcal{H}_a$, so that the state x of the system of equation 5 can be written as

$$x_a = P_a x \qquad (23)$$

Applying P_a to the system of equation (5) and using that $x_a = P_a x$, the system of equation (5) can be approximated by the following N-dimensional ODE system:

$$\left. \begin{array}{r} \dfrac{\mathrm{d}x_a}{\mathrm{d}t} = \mathcal{A}_a(x_a) + \mathcal{B}_a u + f_a(x_a) \\[2mm] y = \mathcal{C}x_a \\[2mm] x_a(0) = P_a x(0) = P_a x_0 \end{array} \right\} \qquad (24)$$

where $\mathcal{A}_a(x_a) = P_a \mathcal{A}(x_a)$, $\mathcal{B}_a = P_a \mathcal{B}$, $f_a(x_a) = P_a f(x_a)$, and $\mathcal{A}_a(x_a), f_a(x_a)$ are Lipschitz vector functions. Proposition 1 that follows establishes a convergence property for the discrepancy between the solutions of the PDE system of equation 5 and the approximation of equation (24), for sufficiently large N. The proof of the proposition is based on standard perturbation arguments and the fact that the solutions of the systems of equations (5) and (24) are assumed to be sufficiently smooth and exponentially stable, and will not be presented for brevity.

Proposition 1: *Consider the system of equation (5) with $u(t) \equiv 0$ and assume that its solution is sufficiently smooth. Suppose also that the system of equation (24) is locally exponentially stable, for any N. Then, there exists an N sufficiently large so that $\forall t \geq 0$*

$$\|x(t) - x_a(t)\|_2 \leq \mu(N) \qquad (25)$$

where $\mu(N)$ is a small positive real number that depends on N and satisfies $\lim_{N \to \infty} \mu(N) = 0$, and $x_a(t)$ is the solution of the system of equation (24) with $u(t) \equiv 0$.

Remark 3: The assumption that the system of equation (24) (and thus, the system of equation (5)) is locally exponentially stable is necessary in order to prove that the estimates of equation (25) hold for all times. When the system of equation (24) is not expo-

nentially stable, one can only prove that the estimates of equation (25) hold for $t \in [0, \tau]$ where τ is a positive real number of $O(1)$.

4.2. *Non-linear Galerkin's method based on singular perturbations*

4.2.1. *Singular perturbation formulation.* The use of linear Galerkin's method for model reduction usually leads (depending on the desired accuracy) to a large-scale discretization of the parabolic PDE system of equation (1) described by the system of equation (24). To reduce further the dimension of the system of equation (24) while preserving the accuracy of the resulting low-dimensional approximation, we take advantage of the fact that the dominant dynamics of parabolic PDE systems are characterized by a small number of degrees of freedom. To quantify this generic property, we initially compute the linearization of the non-linear system of equation (24) around an equilibrium point in the region of interest (which, for simplicity, is assumed to be the origin) to obtain

$$\frac{\mathrm{d}x_a}{\mathrm{d}t} = \mathcal{J}_a x_a + \mathcal{B}_a u \tag{26}$$

where $\mathcal{J}_a$ is the Jacobian of the linearization of the non-linear term $\mathcal{A}_a(x_a) + f_a(x_a)$ around the origin. Using the above linearization, we can rewrite the system of equation (24) as

$$\left. \begin{array}{c} \dfrac{\mathrm{d}x_a}{\mathrm{d}t} = \mathcal{J}_a x_a + \mathcal{B}_a u + \bar{f}_a(x_a) \\[2mm] y = \mathcal{C}x_a \\[2mm] x_a(0) = P_a x(0) = P_a x_0 \end{array} \right\} \tag{27}$$

where $\bar{f}_a(x_a) := \mathcal{A}_a(x_a) + f_a(x_a) - \mathcal{J}_a(x_a)$ is a non-linear vector function which does not include any linear terms. Let $\bar{\lambda}_1, \bar{\lambda}_2, , \bar{\lambda}_N$ be the eigenvalues of $\mathcal{J}_a$ and $\chi_1, \chi_2, \ldots, \chi_N$ be the corresponding eigenvectors, and let $\sigma(\mathcal{J}_a) = \{\bar{\lambda}_1, \ldots, \bar{\lambda}_N\}$ be the eigenspectrum of $\mathcal{J}_a$. Assumption 1 that follows states that the eigenspectrum $\sigma(\mathcal{J}_a)$ can be partitioned into a small set consisting of eigenvalues which are close to the imaginary axis and a finite complement consisting of eigenvalues which are far in the left half of the complex plane (see also Ray 1981, Chen and Chang 1992, Christofides and Daoutidis 1997 for similar assumptions and Remark 4 below for a discussion on the nature of this assumption).

Assumption 1:

(1) $\mathrm{Re}\,\{\bar{\lambda}_1\} \geq \mathrm{Re}\,\{\bar{\lambda}_2\} \geq \cdots \geq \mathrm{Re}\,\{\bar{\lambda}_j\} \geq \cdots,$ where $\mathrm{Re}\,\{\bar{\lambda}_j\}$ denotes the real part of $\bar{\lambda}_j$.

(2) $\sigma(\mathcal{J}_a)$ can be partitioned as $\sigma(\mathcal{J}_a) = \sigma_1(\mathcal{J}_a) + \sigma_2(\mathcal{J}_a)$, where $\sigma_1(\mathcal{J}_a)$ consists of the first m (with m finite) eigenvalues, i.e. $\sigma_1(\mathcal{J}_a) = \{\bar{\lambda}_1, \ldots, \bar{\lambda}_m\}$, and $|\mathrm{Re}\,\{\bar{\lambda}_1\}|/|\mathrm{Re}\,\{\bar{\lambda}_m\}| = O(1)$.

(3) $\mathrm{Re}\,\bar{\lambda}_{m+1} < 0$ and $|\mathrm{Re}\,\{\bar{\lambda}_m\}|/|\mathrm{Re}\,\{\bar{\lambda}_{m+1}\}| = O(\epsilon)$ where $\epsilon := |\mathrm{Re}\,\bar{\lambda}_1|/|\mathrm{Re}\,\bar{\lambda}_{m+1}| < 1$ is a small positive number.

(4) The eigenvectors $\chi_1, \chi_2, \ldots, \chi_N$ are linearly independent.

Defining the matrix $T = [\chi_1 \;\; \chi_2 \;\; \ldots \;\; \chi_N]$ (note that T is an invertible matrix) and using the coordinate change $[x_s^{\mathrm{T}} \; x_f^{\mathrm{T}}]^{\mathrm{T}} = T x_a$, the system of equation (27) can be written as

$$\left. \begin{array}{c} \dfrac{\mathrm{d}x_s}{\mathrm{d}t} = \mathcal{A}_s x_s + \mathcal{B}_s u + \bar{f}_s(x_s, x_f) \\[2mm] \dfrac{\partial x_f}{\partial t} = \mathcal{A}_f x_f + \mathcal{B}_f u + \bar{f}_f(x_s, x_f) \\[2mm] y = \mathcal{C}x_s + \mathcal{C}x_f \\[2mm] x_s(0) = P_s x(0) = P_s x_0, \qquad x_f(0) = P_f x(0) = P_f x_0 \end{array} \right\} \tag{28}$$

where $x_s \in \mathcal{H}_s$, $\quad x_f \in \mathcal{H}_f$ $\quad$ ($\dim(\mathcal{H}_s) + \dim(\mathcal{H}_f) = \dim(\mathcal{H}_a)$), $\mathcal{A}_s$ is a diagonal matrix of dimension $m \times m$ whose elements are $(\bar{\lambda}_1, \ldots, \bar{\lambda}_m)$, $\mathcal{A}_f$ is a diagonal matrix of dimension $(N - m) \times (N - m)$ whose elements are $(\bar{\lambda}_{m+1}, \ldots, \bar{\lambda}_N)$ (this means that $\mathcal{A}_f$ is a stable matrix; it follows from part 3 of assumption 1), and $\mathcal{B}_s, \mathcal{B}_f$ are constant vectors and $\bar{f}_s(x_s, x_f), \bar{f}_f(x_s, x_f)$ are vector functions whose explicit form is omitted for brevity. Using that $\epsilon = |\mathrm{Re}\,\bar{\lambda}_1|/|\mathrm{Re}\,\bar{\lambda}_{m+1}|$, the system of equation (28) can be written in the form:

$$\left. \begin{array}{c} \dfrac{\mathrm{d}x_s}{\mathrm{d}t} = \mathcal{A}_s x_s + \mathcal{B}_s u + \bar{f}_s(x_s, x_f) \\[2mm] \epsilon \dfrac{\partial x_f}{\partial t} = \mathcal{A}_{f\epsilon} x_f + \epsilon \mathcal{B}_f u + \epsilon \bar{f}_f(x_s, x_f) \\[2mm] y = \mathcal{C}x_s + \mathcal{C}x_f \\[2mm] x_s(0) = P_s x(0) = P_s x_0, \qquad x_f(0) = P_f x(0) = P_f x_0 \end{array} \right\} \tag{29}$$

where $\mathcal{A}_{f\epsilon} = \epsilon \mathcal{A}_f$. Since ϵ is a small positive number less than unity (assumption (1), part (3)), the system of equation (29) is in the standard singularly perturbed form, with x_s being the slow states and x_f being the fast states. Defining the fast time-scale $\tau = t/\epsilon$, obtaining the representation of the system of equation (29) in the τ time scale, and setting $\epsilon = 0$, we get the fast subsystem

$$\frac{\partial x_f}{\partial \tau} = \mathcal{A}_{f\epsilon} x_f \tag{30}$$

which is clearly exponentially stable.

Remark 4: Referring to Assumption 1, we note that the assumption of existence of only a few dominant modes that describe the dominant dynamics of the large scale discretizations of a non-linear parabolic PDE system is usually satisfied by the majority of diffusion–reaction processes (Ray 1981, Chen and Chang 1992, Christofides and Daoutidis 1996a). However, this assumption is not satisfied in the cases of: (a) first-order hyperbolic PDE systems (i.e. convection–reaction processes) where the eigenvalues cluster along vertical, or nearly vertical, asymptotes in the complex plane (e.g. Christofides and Daoutidis 1996b), and (b) parabolic PDE systems for which the spatial coordinate is defined in the infinite domain, where the eigenspectrum is continuous and wave-like behaviour is usually exhibited (e.g. Marquardt 1990).

4.2.2. Inertial manifold and approximate inertial manifold. The time-scale multiplicity of the system of equation (29) and the exponential stability of its fast dynamics suggest employing the concept of inertial manifold (Temam 1988) to obtain an *m*-dimensional ODE system which yields solutions that are close, up to a desired accuracy, to the ones of the system of equation (29). Specifically, referring to the system of equation (29), an inertial manifold $\mathcal{M}$, if it exists, is a subset of $\mathcal{H}_a$, which satisfies the following properties (Temam 1988): (i) $\mathcal{M}$ is a finite-dimensional Lipschitz manifold, (ii) $\mathcal{M}$ is a graph of a Lipschitz function $\Sigma(x_s,u,\epsilon)$ mapping $\mathcal{H}_s \times \mathbb{R}^l \times (0,\epsilon^*]$ into $\mathcal{H}_f$ and for every solution $x_s(t),x_f(t)$ of equation (29) with $x_f(0) = \Sigma(x_s(0),u,\epsilon)$, then

$$x_f(t) = \Sigma(x_s(t),u,\epsilon), \qquad \forall\, t \geq 0 \qquad (31)$$

and (iii) $\mathcal{M}$ attracts every trajectory exponentially. The evolution of the state x_f on $\mathcal{M}$ is given by equation (31), while the evolution of the state x_s is governed by the finite-dimensional inertial form

$$\frac{\mathrm{d}x_s}{\mathrm{d}t} = \mathcal{A}_s x_s + \mathcal{B}_s u + \bar{f}_s(x_s, \Sigma(x_s,u,\epsilon)) \qquad (32)$$

Assuming that $u(t)$ is smooth, differentiating equation (31) and utilizing equation (29), $\Sigma(x_s,u,\epsilon)$ can be computed as the solution of the partial differential equation

$$\epsilon\frac{\partial\Sigma}{\partial x_s}[\mathcal{A}_s x_s + \mathcal{B}_s u + \bar{f}_s(x_s,x_f)] + \epsilon\frac{\partial\Sigma}{\partial u}\dot{u}$$
$$= \mathcal{A}_{f\epsilon}x_f + \epsilon\mathcal{B}_f u + \epsilon\bar{f}_f(x_s,x_f) \quad (33)$$

where $x_s \in \mathcal{H}_s$, $u \in \mathbb{R}^l$, $\epsilon \in (0,\epsilon^*]$. From the complexity of equation (33), it is evident that the derivation of an analytic form of $\Sigma(x_s,u,\epsilon)$ is an extremely difficult (if not impossible) task. To overcome the problems associated with the proof of existence of the inertial manifold and the computation of $\Sigma(x_s,u,\epsilon)$, the following standard approximation procedure, which takes advantage

of the two-time-scale property of the system of equation (29), is employed to compute approximations of $\Sigma(x_s,u,\epsilon)$ (approximate inertial manifolds) and approximations of the inertial form, of desired accuracy (see also Kokotovic *et al.* 1986, Christofides and Daoutidis 1997). Consider an expansion of $\Sigma(x_s,u,\epsilon)$ and u in a power series in ϵ:

$$u = \bar{u}_0 + \epsilon\bar{u}_1 + \epsilon^2\bar{u}_2 + \cdots + \epsilon^k\bar{u}_k + O(\epsilon^{k+1})$$

$$\Sigma(x_s,u,\epsilon) = \Sigma^0(x_s,u) + \epsilon\Sigma^1(x_s,u) + \epsilon^2\Sigma^2(x_s,u)$$
$$+ \cdots + \epsilon^k\Sigma^k(x_s,u) + O(\epsilon^{k+1}) \qquad (34)$$

where $\bar{u}_k, \Sigma^k$ are smooth functions. Substituting the expressions of equation (34) into equation (33), and equating terms of the same power in ϵ, one can obtain approximations of $\Sigma(x_s,u,\epsilon)$ up to a desired order. Substituting the expansion for $\Sigma(x_s,u,\epsilon)$ and u up to order k into equation (32), the following approximation of the inertial form is obtained:

$$\frac{\mathrm{d}x_s}{\mathrm{d}t} = \mathcal{A}_s x_s + \mathcal{B}_s(\bar{u}_0 + \epsilon\bar{u}_1 + \epsilon^2\bar{u}_2 + \cdots + \epsilon^k\bar{u}_k)$$
$$+ \bar{f}_s(x_s, \Sigma^0(x_s,u) + \epsilon\Sigma^1(x_s,u) + \epsilon^2\Sigma^2(x_s,u)$$
$$+ \cdots + \epsilon^k\Sigma^k(x_s,u)) \qquad (35)$$

The approach that we used for the derivation of the above *m*-dimensional system is usually referred to as non-linear Galerkin's method. Assuming that the above system is exponentially stable, one can use standard results from singular perturbation theory for finite-dimensional systems (Khalil 1992) (see also Kokotovic *et al.* 1986) to show, that if ϵ is sufficiently small, then the solutions $x_s(t),x_f(t)$ of the system of equation (29) satisfies for all $t \in [t_b,\infty)$

$$\left.\begin{array}{l} x_s(t) = \tilde{x}_s(t) + O(\epsilon^{k+1}) \\ x_f(t) = \tilde{x}_f(t) + O(\epsilon^{k+1}) \end{array}\right\} \qquad (36)$$

where t_b is the time required for $x_f(t)$ to approach $\tilde{x}_f(t)$, $\tilde{x}_s(t)$ is the solution of equation (35) with $u(t) \equiv 0$, and $\tilde{x}_f(t) = \epsilon\Sigma^1(\tilde{x}_s,0) + \epsilon^2\Sigma^2(\tilde{x}_s,0) + \cdots + \epsilon^k\Sigma^k(\tilde{x}_s,0)$. The estimates of equation (25) and equation (36) can be in turn used to characterize the discrepancy between the solution of the open-loop infinite-dimensional system of equation (5), $x(t)$ (and thus, the solution of the parabolic PDE system of equation (1) with $u(t) \equiv 0$) and the solution

$$\tilde{x}_a(t) = T^{-1}[\tilde{x}_s^{\mathrm{T}}(t)\; \tilde{x}_f^{\mathrm{T}}(t)]^{\mathrm{T}}$$
$$= T^{-1}[\tilde{x}_s^{\mathrm{T}}(t)\; (\epsilon\Sigma^1(\tilde{x}_s(t),0)$$
$$+ \cdots + \epsilon^k\Sigma^k(\tilde{x}_s(t),0))^{\mathrm{T}}]^{\mathrm{T}}$$

which is obtained from the $O(\epsilon^k)$ approximation of the open-loop inertial form (i.e. equation (35) with $u(t) \equiv 0$). In particular, substituting equation (36) into the equation $x_a(t) = T^{-1}[x_s^T(t) \; x_f^T(t)]^T$, we have that

$$x_a(t) = T^{-1}[(\tilde{x}_s(t) + O(\epsilon^{k+1}))^T \; (\tilde{x}_f(t) + O(\epsilon^{k+1}))^T]^T$$

$$= \tilde{x}_a(t) + O(\epsilon^{k+1}), \qquad \forall \, t \geq t_b \qquad (37)$$

Utilizing the definition of the order of magnitude and the result of Proposition 1 that $x(t) = x_a(t) + O(\mu(N))$, we finally obtain the following characterization for the discrepancy between $x(t)$ and $\tilde{x}_a(t)$

$$\|x(t) - \tilde{x}_a(t)\|_2 \leq k_1 \epsilon^{k+1} + \mu(N), \qquad \forall \, t \geq t_b \quad (38)$$

where k_1 is a positive real number.

Remark 5: Following the proposed approximation procedure, it can be shown that the $O(\epsilon)$ approximation of $\Sigma(x_s, u, \epsilon)$ is $\Sigma^0(x_s, u) = 0$ and the corresponding approximate inertial form is of the form

$$\left.\begin{aligned} \frac{dx_s}{dt} &= \mathcal{A}_s x_s + \mathcal{B}_s \bar{u}_0 + \bar{f}_s(x_s, 0) \\ y_s &= \mathcal{C} x_s \end{aligned}\right\} \qquad (39)$$

The above system with $\bar{u} \equiv 0$ does not utilize any information about the structure of the fast subsystem, thus yielding solutions which are only $O(\epsilon)$ close to the solutions of the open-loop system of equation (24). On the other hand, the $O(\epsilon^2)$ approximation of $\Sigma(x_s, u, \epsilon)$ can be shown to be of the form

$$\Sigma(x_s, u, \epsilon) = \Sigma^0(x_s, 0) + \epsilon \Sigma^1(x_s, 0)$$

$$= \epsilon(\mathcal{A}_{f\epsilon})^{-1}[-\bar{f}_f(x_s, 0) + \mathcal{B}_f \bar{u}_0] \qquad (40)$$

The corresponding open-loop approximate inertial form has the form

$$\left.\begin{aligned} \frac{dx_s}{dt} &= \mathcal{A}_s x_s + \mathcal{B}_s \bar{u}_0 + \epsilon \mathcal{B}_s \bar{u}_1 \\ &\quad + \bar{f}_s(x_s, (\mathcal{A}_f)^{-1}[-\bar{f}_f(x_s) + \mathcal{B}_f \bar{u}_0]) \\ y_s &= \mathcal{C} x_s + \epsilon \mathcal{C}(\mathcal{A}_{f\epsilon})^{-1}[-\bar{f}_f(x_s, 0) + \mathcal{B}_f \bar{u}_0] \end{aligned}\right\} \qquad (41)$$

The above system does utilize information about the structure of the fast subsystem, and thus allows to obtain solutions which are $O(\epsilon^2)$ close to the solutions of the open-loop system of equation (24).

Remark 6: We point out that when the approximate ODE model of equation (35) is obtained through non-linear Galerkin's method with *empirical eigenfunctions*, it provides a valid approximation of the parabolic PDE model in a broad region of the state space and not only in the region that was used for the computation of the snapshots, provided that the ensemble of

snapshots is sufficiently large and contains sufficient information of the global dynamics of the PDE system. This property is a consequence of the fact that the empirical eigenfunctions form an orthogonal set of functions whose dimension is equal to the number of snapshots, and thus, it can be made arbitrarily large (even though completeness of this set cannot be guaranteed). Therefore, the computation of approximate ODE models through Galerkin's method with empirical eigenfunctions is conceptually similar to the computation of ODE models through Galerkin's method with other standard basis functions sets (sine and cosine functions, Legendre polynomials, etc.), and thus, the result of Proposition 1 guarantees the convergence of the finite-dimensional approximation when empirical eigenfunctions are used, as long as the ensemble of snapshots is sufficiently representative and large. Finally, the major practical benefit of using empirical eigenfunctions is that they directly satisfy the boundary conditions of the PDE system; a very important property for the case of PDEs with non-linear boundary conditions (see, for example, the RTCVD process considered in §4).

5. Finite-dimensional non-linear control

In this section, we initially synthesize a finite-dimensional non-linear output feedback controller on the basis of the system of equation (35) that guarantees stability and enforces output tracking in the closed-loop ODE system. Then, the estimates of equation (36) are used to establish that the same controller also exponentially stabilizes the closed-loop PDE system and ensures that the discrepancy between the output of the closed-loop ODE system and the output of the closed-loop PDE system is of $O(\epsilon^{k+1} + \mu(N))$, provided that ϵ is sufficiently small.

The controller is constructed through a standard combination of a state feedback controller with a state observer. In particular, we consider a state feedback control law of the general form

$$u = \bar{u}_0 + \epsilon \bar{u}_1 + \cdots + \epsilon^k \bar{u}_k$$

$$= p_0(x_s) + Q_0(x_s)v + \epsilon[p_1(x_s) + Q_1(x_s)v]$$

$$+ \cdots + \epsilon^k[p_k(x_s) + Q_k(x_s)v] \qquad (42)$$

where $p_0(x_s), \ldots, p_k(x_s)$ are smooth vector functions, $Q_0(x_s), \ldots, Q_k(x_s)$ are smooth matrices, and $v \in \mathbb{R}^l$ is the constant reference input vector. The state feedback law of equation (42) will be constructed by following a sequential procedure to enforce stability and output tracking in the $O(\epsilon^{k+1})$ approximation of the closed-loop inertial form. Specifically, the component $\bar{u}_0 = p_0(x_s) + Q_0(x_s)v$ will be initially synthesized on

the basis of the $O(\epsilon)$ approximation of the inertial form; then the component $\bar{u}_1 = p_1(x_s) + Q_1(x_s)v$ will be synthesized on the basis of the $O(\epsilon^2)$ approximation of the inertial form. In general, at the k-th step, the component $\bar{u}_k = p_k(x_s) + Q_k(x_s)v$ will be synthesized on the basis of the $O(\epsilon^{k+1})$ approximation of the inertial form (equation (35)). The synthesis of $[p_\nu(x_s), Q_\nu(x_s)]$, $\nu = 0, \ldots, k$, will be performed, at each step, utilizing standard geometric control methods for non-linear ODEs (Isidori 1989) (see Theorem 1 below for an explicit controller synthesis formula).

The following m-dimensional state observer is also considered for the implementation of the state feedback law of equation (42):

$$\frac{\mathrm{d}\eta}{\mathrm{d}t} = \mathcal{A}_s\eta + \mathcal{B}_s(p_0(\eta) + Q_0(\eta)v + \epsilon[p_1(\eta) + Q_1(\eta)v]$$

$$+ \cdots + \epsilon^k[p_k(\eta) + Q_k(\eta)v])$$

$$+ f_s(\eta, \epsilon\Sigma^1(\eta,u) + \epsilon^2\Sigma^2(\eta,u) + \cdots + \epsilon^k\Sigma^k(\eta,u))$$

$$+ L(y - [\mathcal{C}\eta + \mathcal{C}\{\epsilon\Sigma^1(\eta,u) + \epsilon^2\Sigma^2(\eta,u)$$

$$+ \cdots + \epsilon^k\Sigma^k(\eta,u)\}]) \tag{43}$$

where $\eta \in \mathcal{H}_s$ denotes the observer state vector, and L is a matrix chosen so that the eigenvalues of the matrix

$$C_L = \mathcal{A}_s + \left(\frac{\partial f_s}{\partial \eta}\right)_{(\eta=\eta_s)}$$

$$- L\left[\mathcal{C}\eta_s + \mathcal{C}\left\{\frac{\partial}{\partial\eta}(\epsilon\Sigma^1(\eta,u(\eta)) + \epsilon^2\Sigma^2(\eta,u(\eta))\right.\right.$$

$$\left.\left. + \cdots + \epsilon^k\Sigma^k(\eta,u(\eta)))_{(\eta=\eta_s)}\right\}\right]$$

lie in the open left-half of the complex plane, where η_s denotes the steady-state for the system of equation (43).

Theorem 1 below provides the synthesis formula of the output feedback controller and conditions that guarantee closed-loop stability in the case of considering an $O(\epsilon^2)$ approximation of the exact slow system for the synthesis of the controller. The derivation of synthesis formulas for higher-order approximations of the output feedback controller is notationally complicated, although conceptually straightforward, and thus will be omitted for reasons of brevity. In order to simplify the statement of the theorem, we set $\mathcal{A}_s x_s + f_s(x_s, 0) = f_0(x_s)$, $\mathcal{B}_s = g_0$, $\mathcal{C}x_s = h_0(x_s)$, $\mathcal{A}_s x_s + \mathcal{B}_s u_0 + f_s(x_s, (\mathcal{A}_f)^{-1}[-\bar{f}_f(x_s) + \mathcal{B}_f \bar{a}_0]) = f_1(x_s, \epsilon)$, $\epsilon\mathcal{B}_s = g_1(x_s, \epsilon)$, and $\mathcal{C}x_s + \mathcal{C}\epsilon(\mathcal{A}_{f\epsilon})^{-1}[-\bar{f}_f(x_s, 0) + \mathcal{B}_f \bar{a}_0] = h_1(x_s, \epsilon)$. Fur-

thermore, referring to the system of equation (39), we define the relative order of the output y_s^i with respect to the vector of manipulated inputs u as the smallest integer r_i for which

$$[L_{g_0^1}L_{f_0}^{r_i-1}h_0^i(x_s) \quad \cdots \quad L_{g_0^l}L_{f_0}^{r_i-1}h_0^i(x_s)] \not\equiv [0 \quad \cdots \quad 0] \tag{44}$$

or $r_i = \infty$ if such an integer does not exist, and the characteristic matrix

$$C_0(x_s) = \begin{bmatrix} L_{g_0^1}L_{f_0}^{r_1-1}h_0^1(x_s) & \cdots & L_{g_0^l}L_{f_0}^{r_1-1}h_0^1(x_s) \\ L_{g_0^1}L_{f_0}^{r_2-1}h_0^2(x_s) & \cdots & L_{g_0^l}L_{f_0}^{r_2-1}h_0^2(x_s) \\ \vdots & & \\ L_{g_0^1}L_{f_0}^{r_l-1}h_0^l(x_s) & \cdots & L_{g_0^l}L_{f_0}^{r_l-1}h_0^l(x_s) \end{bmatrix} \tag{45}$$

One can similarly define the characteristic matrix, $C_1(\eta,\epsilon)$, for the system of equation (41) (the explicit form of $C_1(\eta,\epsilon)$ is omitted for brevity).

Theorem 1: *Consider the parabolic PDE system of equation* (5), *for which Assumption* 1 *holds. Consider also the $O(\epsilon^2)$ approximation of the inertial form, and assume that its characteristic matrix $C_1(x_s,\epsilon)$ is invertible $\forall x_s \in \mathcal{H}_s$, $\epsilon \in [0, \epsilon^*]$. Suppose also that the following conditions hold:* (1) *the roots of the equation* $\det(B(s)) = 0$ *where $B(s)$ is an $l \times l$ matrix, whose (i,j)th element is of the form $\sum_{k=0}^{r_i} \beta_{jk}^i s^k$, lie in the open left-half of the complex plane, and* (2) *the unforced $(v \equiv 0)$ zero dynamics of the $O(\epsilon^2)$ approximation of the inertial form is locally exponentially stable. Then, there exist constants μ_1, μ_2, ϵ^* such that if $|x_s(0)| \leq \mu_1$, $\|x_f(0)\|_2 \leq \mu_2$ and $\epsilon \in (0, \epsilon^*]$, then if $\eta(0) = x_s(0)$, the dynamic output feedback controller*

$$\frac{\mathrm{d}\eta}{\mathrm{d}t} = \mathcal{A}_s\eta + \mathcal{B}_s(p_0(\eta) + Q_0(\eta)v + \epsilon[p_1(\eta) + Q_1(\eta)v])$$

$$+ f_s(\eta, \epsilon\Sigma^1(\eta,u)) + L(y - [\mathcal{C}\eta + \mathcal{C}\{\Sigma^0(\eta,u)$$

$$+ \epsilon\Sigma^1(\eta,u)\}])$$

$$u = p_0(\eta) + Q_0(\eta)v + \epsilon[p_1(\eta) + Q_1(\eta)v]$$

$$:= \left\{[\beta_{1r_1} \quad \cdots \quad \beta_{lr_l}]C_0(\eta)\right\}^{-1}\left\{v - \sum_{i=1}^{l}\sum_{k=0}^{r_i}\beta_{ik}L_{f_0}^k h_0^i(\eta)\right\}$$

$$+ \epsilon\left\{[\beta_{1r_1} \quad \cdots \quad \beta_{lr_l}]C_1(\eta,\epsilon)\right\}^{-1}$$

$$\times \left\{v - \sum_{i=1}^{l}\sum_{k=0}^{r_i}\beta_{ik}L_{f_1}^k h_1^i(\eta,\epsilon)\right\}$$

(a) *guarantees exponential stability of the closed-loop system, and*

(b) *ensures that the outputs of the closed-loop system satisfy for all $t \in [t_b, \infty)$*

$$y^i(t) = y_s^i(t) + O(\epsilon^2 + \mu(N)), \qquad i = 1, \ldots, l \quad (47)$$

where t_b is the time required for the off-manifold fast transients to decay to zero exponentially, and $y_s^i(t)$ is the solution of

$$\sum_{i=1}^{l} \sum_{k=0}^{r_i} \beta_{ik} \frac{\mathrm{d}^k y_s^i}{\mathrm{d}t^k} = v, \qquad i = 1, \ldots, l \quad (48)$$

Proof of theorem 1: Substituting the output feedback controller of equation (46) into the infinite dimensional system of equation (5), we get

$$\left.\begin{aligned}
\frac{\mathrm{d}\eta}{\mathrm{d}t} &= \mathcal{A}_s\eta + \mathcal{B}_s(p_0(\eta) + Q_0(\eta)v + \epsilon[p_1(\eta) + Q_1(\eta)v]) \\
&\quad + \bar{f}_s(\eta, \epsilon\Sigma_1(\eta, \bar{u}_0)) + L(\mathcal{C}x_s + \mathcal{C}x_f - \mathcal{C}\eta \\
&\quad - \epsilon\mathcal{C}\Sigma_1(\eta, \bar{u}_0)) \\
\dot{x} &= \mathcal{A}(x) + \mathcal{B}(p_0(\eta) + Q_0(\eta)v + \epsilon[p_1(\eta) + Q_1(\eta)v]) \\
&\quad + f(x) \\
y &= \mathcal{C}x
\end{aligned}\right\} \quad (49)$$

where $\bar{u}_0 = p_0(\eta) + Q_0(\eta)v$. Applying Galerkin's method to the x-subsystem of the above set of equations and using the linearization of equation (26), we obtain

$$\left.\begin{aligned}
\frac{\mathrm{d}\eta}{\mathrm{d}t} &= \mathcal{A}_s\eta + \mathcal{B}_s(p_0(\eta) + Q_0(\eta)v + \epsilon[p_1(\eta) + Q_1(\eta)v]) \\
&\quad + \bar{f}_s(\eta, \epsilon\Sigma_1(\eta, \bar{u}_0)) + L(\mathcal{C}x_s + \mathcal{C}x_f - \mathcal{C}\eta \\
&\quad - \epsilon\mathcal{C}\Sigma_1(\eta, \bar{u}_0)) \\
\frac{\mathrm{d}x_a}{\mathrm{d}t} &= \mathcal{J}_a x_a + \mathcal{B}_a(p_0(\eta) + Q_0(\eta)v + \epsilon[p_1(\eta) + Q_1(\eta)v]) \\
&\quad + \bar{f}_a(x_a) \\
y &= \mathcal{C}x_a
\end{aligned}\right\} \quad (50)$$

Since the matrix $\mathcal{J}_a$ satisfies the properties of Assumption 1, the above system can be directly written in the singularly perturbed form

$$\left.\begin{aligned}
\frac{\mathrm{d}\eta}{\mathrm{d}t} &= \mathcal{A}_s\eta + \mathcal{B}_s(p_0(\eta) + Q_0(\eta)v + \epsilon[p_1(\eta) + Q_1(\eta)v]) \\
&\quad + \bar{f}_s(\eta, \epsilon\Sigma_1(\eta, \bar{u}_0)) + L(\mathcal{C}x_s + \mathcal{C}x_f - \mathcal{C}\eta \\
&\quad - \epsilon\mathcal{C}\Sigma_1(\eta, \bar{u}_0)) \\
\frac{\mathrm{d}x_s}{\mathrm{d}t} &= \mathcal{A}_s x_s + \mathcal{B}_s(p_0(\eta) + Q_0(\eta)v + \epsilon[p_1(\eta) + Q_1(\eta)v]) \\
&\quad + \bar{f}_s(x_s, x_f) \\
\epsilon\frac{\partial x_f}{\partial t} &= \mathcal{A}_{f\epsilon}x_f + \epsilon\mathcal{B}_f(p_0(\eta) + Q_0(\eta)v + \epsilon[p_1(\eta) \\
&\quad + Q_1(\eta)v]) + \epsilon\bar{f}_f(x_s, x_f) \\
y &= \mathcal{C}x_s + \mathcal{C}x_f
\end{aligned}\right\} \quad (51)$$

Performing a two-time-scale decomposition in the above system, the fast subsystem takes the form

$$\frac{\partial x_f}{\partial \tau} = \mathcal{A}_{f\epsilon}x_f \quad (52)$$

which is exponentially stable (Assumption 1; part (3)). The $O(\epsilon^2)$ approximation of the closed-loop inertial form is

$$\left.\begin{aligned}
\frac{\mathrm{d}\eta}{\mathrm{d}t} &= \mathcal{A}_s\eta + \mathcal{B}_s(p_0(\eta) + Q_0(\eta)v + \epsilon[p_1(\eta) + Q_1(\eta)v]) \\
&\quad + \bar{f}_s(\eta, \epsilon\Sigma_1(\eta, \bar{u}_0)) + L(\mathcal{C}x_s + \epsilon\mathcal{C}\Sigma_1(x_s, \bar{u}_0) - \mathcal{C}\eta \\
&\quad - \epsilon\mathcal{C}\Sigma_1(\eta, \bar{u}_0)) \\
\frac{\mathrm{d}x_s}{\mathrm{d}t} &= \mathcal{A}_s x_s + \mathcal{B}_s(p_0(\eta) + Q_0(\eta)v + \epsilon[p_1(\eta) + Q_1(\eta)v]) \\
&\quad + \bar{f}_s(x_s, \epsilon\Sigma_1(x_s, \bar{u}_0)) \\
y_s^i &= \mathcal{C}^i x_s + \epsilon\mathcal{C}^i\Sigma_1(x_s, \bar{u}_0), \quad i = 1, \ldots, l
\end{aligned}\right\} \quad (53)$$

Using the hypothesis $\eta(0) = x_s(0)$, the above system can be written as

$$\left.\begin{aligned}
\frac{\mathrm{d}x_s}{\mathrm{d}t} &= \mathcal{A}_s x_s + \mathcal{B}_s(p_0(x_s) + Q_0(x_s)v + \epsilon[p_1(x_s) \\
&\quad + Q_1(x_s)v]) + \bar{f}_s(x_s, \epsilon\Sigma_1(x_s, \bar{u}_0)) \\
y_s^i &= \mathcal{C}^i x_s + \epsilon\mathcal{C}^i\Sigma_1(x_s, \bar{u}_0), \qquad i = 1, \ldots, l
\end{aligned}\right\} \quad (54)$$

where $\bar{u}_0 = p_0(x_s) + Q_0(x_s)v$. Computing the time-derivatives of the controlled output y_s^i up to order r_i and substituting into equation (48), one can show that the input/output response of equation (48) is enforced in the above closed-loop system. Furthermore, an approach, similar to the one in

Isidori (1989), can be followed to establish that Assumptions 1 and 2 of the theorem guarantee that the system of equation (54) is locally exponentially stable. Therefore, we have that the system of equation (53) is locally exponentially stable and its outputs y_s^i, $i = 1, \ldots, l$, change according to equation (48). A direct application of the estimates of equation (34) then yields that there exist positive real numbers μ_1, μ_2, ϵ^* such that if $|x_s(0)| \leq \mu_1$, $\|x_f(0)\|_2 \leq \mu_2$ and $\epsilon \in (0, \epsilon^*]$, the closed-loop infinite-dimensional system is exponentially stable and the relation of equation (47) holds. $\square$

Remark 7: The exponential stability of the closed-loop system guarantees that in the presence of small errors in process parameters, the states of the closed-loop system will be bounded. Furthermore, since the input/output spaces of the closed-loop system are finite dimensional, and the controller of equation (46) enforces a linear input/output dynamics between y and v, it is possible to implement a linear error feedback controller around the $(y - v)$ loop to ensure asymptotic offsetless output tracking in the closed-loop system, in the presence of constant unknown process parameters and unmeasured disturbance inputs.

Remark 8: We note that the approach followed here for the synthesis of finite-dimensional controllers is not directly applicable to hyperbolic PDE systems where the eigenvalues cluster along vertical or nearly vertical asymptotes in the complex plane and thus, the controller has to be modified to compensate for the destabilizing effect of the residual modes (Balas 1991).

Remark 9: Note that in the case of imperfect initialization of the observer states (i.e. $\eta(0) \neq x_s(0)$), although a slight deterioration of the performance may occur (i.e. the requirement of equation (47) will not be exactly imposed in the closed-loop system), the output feedback controller of Theorem 1 guarantees exponential stability and asymptotic output tracking in the closed-loop system.

6. Non-linear model reduction and control of rapid thermal chemical vapour deposition

We consider a low pressure rapid thermal chemical vapour deposition (RTCVD) process shown in figure 1. This process closely resembles an experimental RTCVD reactor located at the North Carolina State University Center for Advanced Electronic Materials Processing (Kiether *et al.* 1994). The process consists of a quartz chamber, three banks of tungsten heating lamps which are used to heat the wafer and a fan which is located at the bottom of the reactor and is used to cool the chamber. The furnace is designed so that the top lamp bank *A* and the bottom lamp bank *C* heat the total area of the wafer, while the lamp bank *B*, which surrounds the reac-
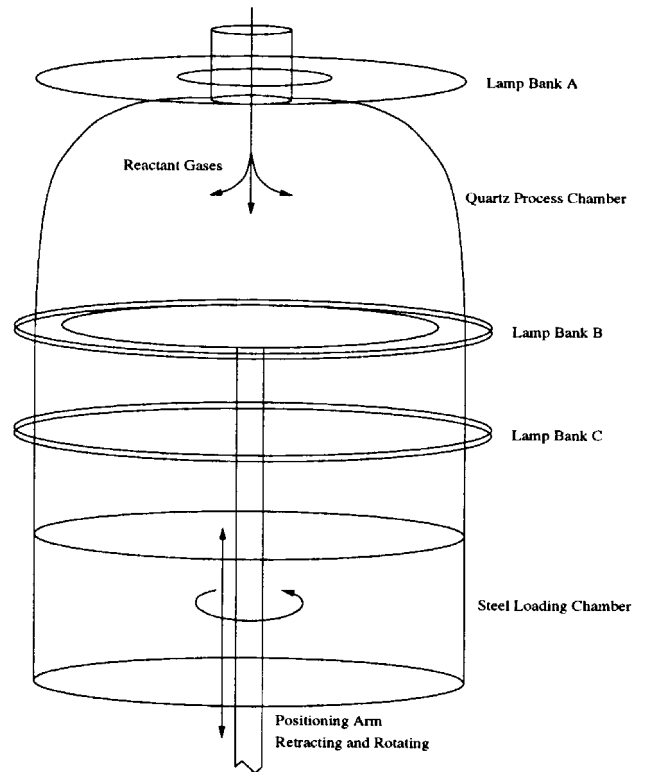

Figure 1. A rapid thermal chemical vapour deposition process.

tor, is used to heat the wafer edge in order to compensate for heat loss that occurs from the edge (radiative cooling between wafer edge and quartz chamber). The wafer is rotated while heated for azimuthal temperature uniformity. A small opening exists on the top of the quartz chamber which is used to feed the reacting gases. The objective of the process is to deposit a $0.5\,\mu m$ film of polycrystalline silicon on a 6-inch wafer in 40 s. To achieve this objective, the reactor is fed with 10% SiH_4 in Ar at 5 torr pressure and the heating lamps are used to heat the wafer from room temperature to 1200 K (this is the temperature where the deposition reactions take place), at a heating rate of the order of 180 K/s.

In order to develop a non-linear model-based feedback controller for the RTCVD process, we initially consider a detailed mathematical model for the process which is similar to the one used in Theodoropoulou *et al.* (1998) (see also Breedijk *et al.* 1993) and is based on the following standard assumptions

(1) Wafer temperature uniformity in the azimuthal direction due to wafer rotation and symmetric reactor design.

(2) Negligible wafer temperature variations in the axial direction due to small thickness of the wafer.

(3) Negligible heat transfer from the wafer to the reactant gases due to low pressure conditions inside the chamber.

(4) Negligible heat of deposition reactions compared to radiative heat transfer from the lamps to the wafer.

(5) Constant optical properties of the wafer and the chamber.

(6) Perfect mixing of the reacting mixture.

(7) Spatially uniform quartz chamber wall thermal dynamics.

Under the above assumptions an energy balance on the wafer yields the non-linear parabolic PDE

$$\rho_w T_{amb} \frac{\partial}{\partial t}(C_{p_w}(T)T) = \frac{T_{amb}}{R_w^2} \frac{1}{r} \frac{\partial}{\partial r}\left(\kappa(T)r\frac{\partial T}{\partial r}\right)$$
$$- \frac{q_{rad}(T,r)}{\delta z} \quad (55)$$

subject to the boundary conditions

$$\left.\frac{\partial T}{\partial r}\right|_{r=0} = 0 \quad (56)$$

$$\left.\left(\kappa(T)\frac{\partial T}{\partial r}\right)\right|_{r=1} = -\sigma\epsilon_w T_{amb}^4(T^4 - T_c^4) + q_{edge}u_b \quad (57)$$

In the above equations, T_{amb} denotes the ambient temperature, $T = T'/T_{amb}$ denotes the dimensionless wafer temperature, ρ_w, C_{p_w}, R_w denote the density, heat capacity and radius of the wafer, $r = r'/R_w$ denotes the dimensionless radial coordinate, q_{rad} is a term that accounts for radiative energy transfer between the wafer and its environment (see below for an explicit statement of the radiative phenomena contributing to this term), $T_c = T'_c/T_{amb}$ denotes the dimensionless temperature of the chamber, σ denotes the Boltzmann constant, ϵ_w denotes the emissivity of the wafer, q_{edge} denotes the energy flux at the edge of the wafer and u_b denotes the percentage of the side lamp power that is used. The wafer heat capacity and thermal conductivity depend on temperature according to the relations

$$\left.\begin{aligned} \kappa(T) &= 50.5\ln\left(TT_{amb}\right)^2 - 734.0\ln\left(TT_{amb}\right) \\ &\quad + 2.69\times10^3 \text{ W/m K} \\ C_{p_w}(T) &= 1.06\times10^3 - 1.04\times10^5/(TT_{amb}) \text{ J/(Kg K)} \end{aligned}\right\} \quad (58)$$

The radiative energy transfer term q_{rad} consists of two parts: the radiant energy absorbed from the heating lamps and the radiant energy exchanged between the wafer and reactor walls, i.e.

$$q_{rad} = -Q_{lamps,w} \cdot u + q_{dw,t} + q_{dw,b} \quad (59)$$

where $Q_{lamps,w}$ is a vector of the total energy emitted from the three lamp banks and absorbed by the wafer, $u = [u_A u_B u_C]$ is the percentage of the lamp power that is used, $q_{dw,t}$ ($q_{dw,b}$) is the net radiative energy transferred to the wafer top (bottom) surface from sources other than the lamps. The heating lamp energy flux to the wafer surface, $Q_{lamps,w}$, is computed by a ray-trace algorithm, which calculates the radiant energy flux distributions directly from the lamps to the wafer as well as the contribution of reflected arrays. The radiant energy flux distribution for each lamp bank as a function of wafer radial position can be found in Theodoropoulou *et al.* (1998). The radiation exchange between the wafer and the walls (terms $q_{dw,t}$ and $q_{dw,b}$) is computed using the net-radiation method. We note that $q_{dw,t}, q_{dw,b}$ are highly non-linear functions of the wafer and chamber temperatures, geometry of the reactor and emissivity of wafer and chamber.

An energy balance on the quartz chamber yields the ordinary differential equation

$$T_{amb} M_c \frac{dT_c}{dt} = \epsilon_c Q_{lamps} \cdot u - A_{hem} q_h - A_{cyl} q_c$$
$$- Q_{convect} - \sigma\epsilon_c A_c T_{amb}^4(T_c^4 - 1) \quad (60)$$

where M_c denotes the chamber thermal mass, ϵ_c denotes the emissivity of the chamber, A_{hem} denotes the chamber hemispherical area, A_{cyl} denotes the chamber cylindrical area and A_c denotes the chamber outside area. q_h and q_c denote the net energy radiated from the hemispherical and cylindrical portions of the quartz chamber, respectively, and their expressions computed from the net-radiation method can be found in Theodoropoulou *et al.* (1998). The term $Q_{lamps} \cdot u$ represents energy absorbed by the chamber directly from the heating lamps, while $Q_{convect}$ denotes the energy transferred from the quartz chamber to the cooling gas by forced convective cooling. The explicit computation of $Q_{convect}$ can be done by a simple cooling gas energy balance and is given in Theodoropoulou *et al.* (1998).

The assumption of perfect mixing of the reacting mixture allows us to derive the following set of ODEs which describe the time evolution of the molar fraction of SiH_4, X_{SiH_4}, and hydrogen, X_{H_2}

$$\left.\begin{aligned} \frac{dX_{SiH_4}}{dt} &= -\alpha\int_{A_w} R_s(T,X_{SiH_4},X_{H_2})\,dA_w \\ &\quad + \frac{1}{\tau}(X_{SiH_4}^{in} - X_{SiH_4}) \\ \frac{dX_{H_2}}{dt} &= 2\alpha\int_{A_w} R_s(T,X_{SiH_4},X_{H_2})\,dA_w - \frac{1}{\tau}X_{H_2} \end{aligned}\right\} \quad (61)$$

where α is the mole to mole conversion factor, A_w is the wafer area, τ is the residence time, $X_{SiH_4}^{in}$ is the molar fraction of SiH_4 in the inlet stream to the reactor and R_s is the rate of the deposition reactions

$$R_s(T, X_{SiH_4}, X_{H_2}) = \frac{k_0 \, \exp\left(-\gamma/RT \, T_{amb}\right)X_{SiH_4}P_{tot}}{1 + bX_{SiH_4}P_{tot} + \sqrt{X_{H_2}P_{tot}}/c} \tag{62}$$

where k_0 is the pre-exponential constant, γ is the activation energy for deposition, P_{tot} is the total pressure and b, c are constants. The deposition rate of Si onto the wafer surface is governed by the expression:

$$\frac{dS}{dt} = \frac{MW_{Si}}{\rho_{Si}}R_s(T, X_{SiH_4}, X_{H_2}) \tag{63}$$

where MW_{Si} and ρ_{Si} denote the molecular weight and density of Si, respectively. Note the Arrhenius dependence of the deposition rate on wafer temperature in equation (63) which means that non-uniform temperature results in non-uniform deposition, thereby implying the need to develop and implement a non-linear feedback controller on the process in order to achieve radially uniform wafer temperature.

We now turn to the application of the proposed model reduction and output feedback control methods to the RTCVD process. The values of the process parameters used in the simulations are given in table 1. A second-order finite difference scheme with 100 discretization points was initially used to compute an accurate solution of the model of the RTCVD process (equations (55), (60) and (61)). For time integration, the Euler method was used. Following Theodoropoulou *et al.* (1998), the non-linear boundary condition of equation (57) was solved simultaneously at each time step using a Gauss–Newton method. We found through extensive simulation runs of the open-loop process model that the solution of the process exists and is well-defined for a wide range of operating conditions. A 40 s simulation run of the process with the following initial conditions: $T = 1$, $T_c = 1$, $S = 0$, $X_{SiH_4} = 0.1$ and $X_{H_2} = 0$ was used to compute 600 snapshots of the wafer temperature profile. The deviations of these snapshots from a mean spatially uniform wafer temperature profile were used as data for determining the dominant spatial temperature modes (wafer temperature empirical eigenfunctions) through Karhunen–Loéve expansion. The first three empirical eigenfunctions (denoted by ϕ_2, ϕ_3 and ϕ_4, respectively) computed via Karhunen–Loéve expansion are shown in figure 2. Since we analysed temperature profile deviations, the first eigenfunction was taken to be a spatially uniform one. We also found that the first three empirical eigenfunctions account for more than 99.0% of the energy contained in the ensemble

Table 1. Process parameters

$A_2 = 182.41 \times 10^{-4}$	m^2
$A_c = 1217.31 \times 10^{-4}$	m^2
$A_{cyl} = 794.83 \times 10^{-4}$	m^2
$A_{hem} = 422.48 \times 10^{-4}$	m^2
$L_c = 15.43 \times 10^{-2}$	m
$L_s = 10 \times 10^{-2}$	m
$R_c = 8.2 \times 10^{-2}$	m
$R_w = 7.62 \times 10^{-2}$	m
$\delta z = 0.05 \times 10^{-2}$	m
$M_c = 1422.6$	$J\,K^{-1}$
$q_{edge} = 49 \times 10^4$	$J\,s^{-1}\,m^{-2}$
$b = 78.95$	$torr^{-1}$
$c = 0.38$	$torr^{1/2}$
$e_w = 0.7$	
$e_c = 0.37$	
$\rho_c = 2.6433 \times 10^3$	$kg\,m^{-3}$
$V_c = 638.25 \times 10^6$	m^3
$\rho_w = 2.3 \times 10^3$	$kg\,m^{-3}$
$X_{SiH_4}^{in} = 0.1$	$kmol_{SiH_4}\,kmol_{feed}^{-1}$
$P_{tot} = 5.0$	torr
$MW_{Si} = 28.086$	$kg\,kmol^{-1}$
$\rho_{Si} = 2.3 \times 10^3$	$kg\,m^{-3}$
$R = 8.314 \times 10^3$	$J\,kmol^{-1}\,K^{-1}$
$T_{amb} = 300.0$	K
$\alpha = 12.961 \times 10^6$	$kmol^{-1}$
$k_0 = 263.158 \times 10^1$	$kmol\,m^{-2}\,s^{-1}\,torr^{-1}$
$\gamma = 153.809 \times 10^6$	$J\,kmol^{-1}$
$\sigma = 5.6705 \times 10^{-8}$	$J\,s^{-1}\,m^{-2}\,K^{-4}$
$\tau = 0.380$	s

of snapshots (i.e. $\lambda_2 + \lambda_3 + \lambda_4 \geq 0.99$, when $\lambda_2 + \cdots + \lambda_{\kappa+1} = 1$ where $\kappa = 600$ is the number of snapshots).

Then, a collocation formulation of Galerkin's method was used to obtain a low-order model that describes the wafer temperature. The wafer temperature was expanded in terms of four global basis functions: one spatially uniform function plus the three empirical eigenfunctions of figure 2. The three roots of the fourth empirical eigenfunction were used as collocation points, thereby forcing the residual to be orthogonal, and therefore zero, at these points. Additional collocation points were added at $r = 0$ and $r = 1$ to satisfy the boundary conditions. Therefore, the dimension of the constructed low-order model was five. In order to test the validity of the low-order model, simulations of the detailed and low-order models were performed by using an open-loop recipe (obtained from a trial and error procedure) to manipulate the power of the top lamps in order to heat the wafer from room temperature to 1200 K. The wafer temperature profiles obtained by the detailed and low-order models, and their difference at all positions and times, are shown in figure 3. Clearly, the predictive capabilities of the low-order model are excellent.

The fifth-order model obtained above was used to synthesize a non-linear multivariable output feedback
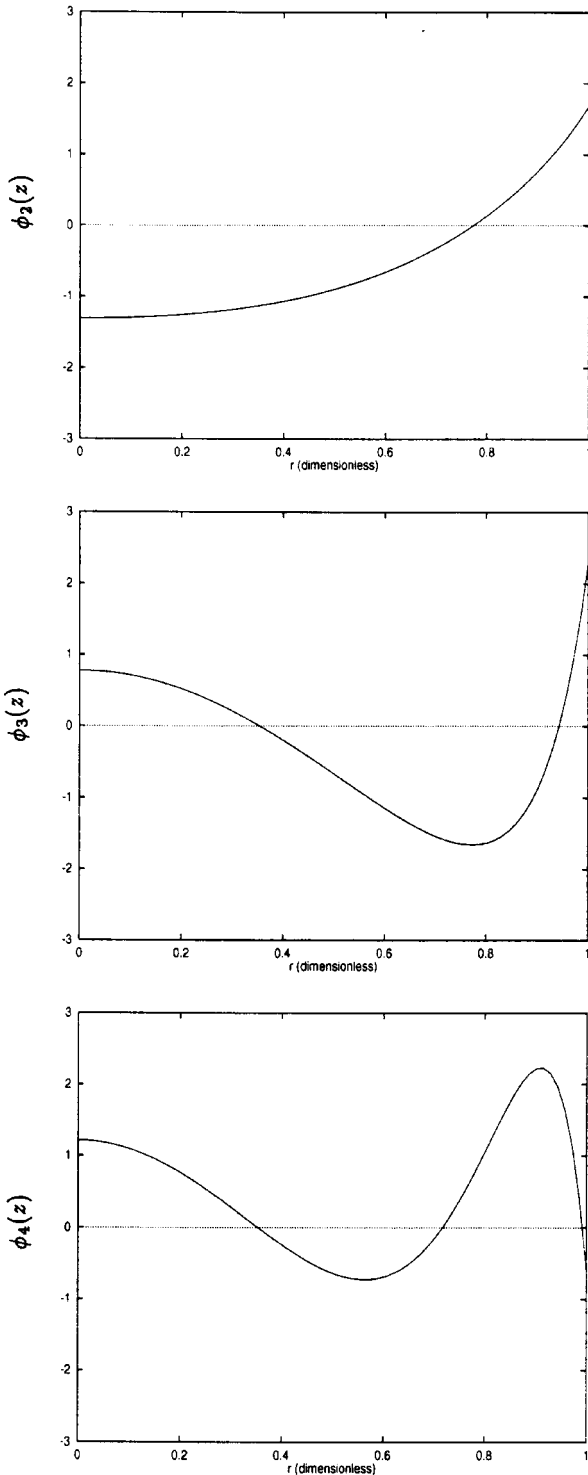
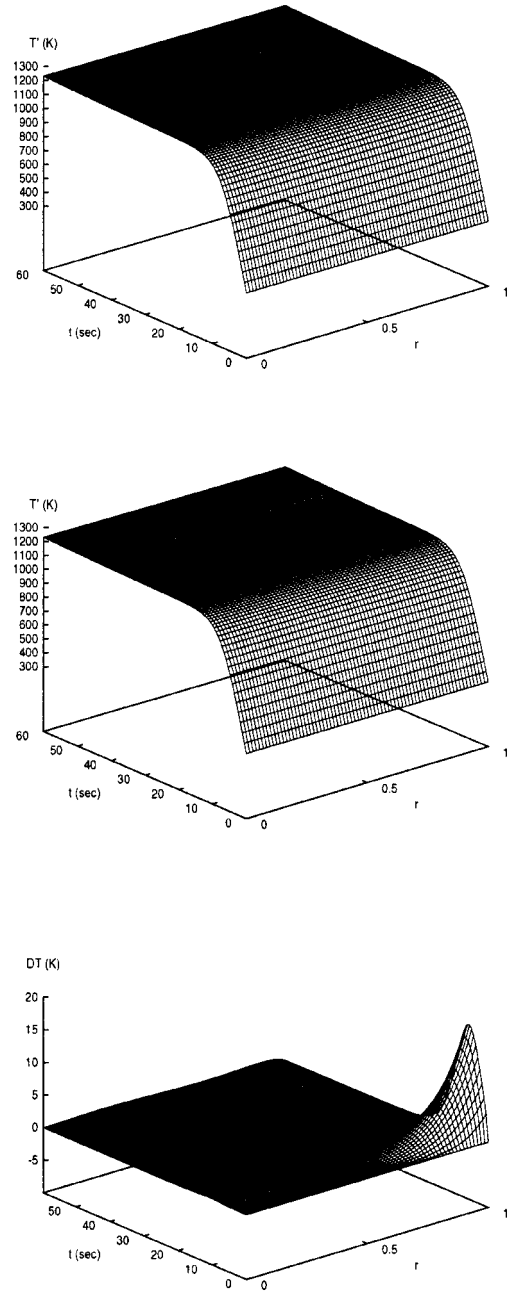Figure 2.   First three empirical eigenfunctions.

Figure 3.   Spatiotemporal wafer temperature profiles—full model (top figure), reduced-order model (middle figure), difference between full and reduced-order models (bottom figure).

controller using the controller synthesis formula of theorem 1 with $\epsilon = 0$. The controller uses measurements of the wafer temperature at five locations across the wafer and adjusts the power of the top lamp (the top lamp is assumed to be divided into four equispaced concentric independently-controlled lamps; see figure 4 for a

schematic of the control configuration) to control the temperature at the four interior collocation points. A simulation run was performed to evaluate the performance of the non-linear controller for a 40 s cycle with initial conditions: $T = 1$, $T_c = 1$, $S = 0$, $X_{SiH_4} = 0.1$ and $X_{H_2} = 0$. Figure 5 shows the spatiotemporal evolution of the wafer temperature (top plot), the temperature
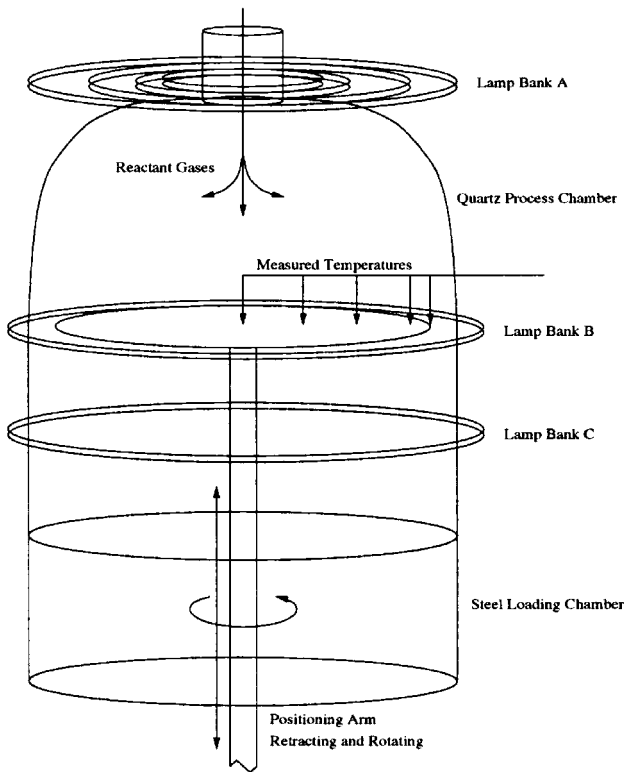
Figure 4. Control problem specification for rapid thermal chemical vapour deposition process.

distribution along the radius of the wafer at $t = 40\,\mathrm{s}$ (middle plot), and the thickness of the deposition (bottom plot). The profiles of the four manipulated inputs are shown in figure 6 (note that $u_i(t) = (\text{Power in } i\text{th}$ concentric region of the top lamp)/(5000 W)). The performance of the non-linear controller is excellent, achieving an almost uniform (less than 1% variation) thin film deposition. For the sake of comparison, we also implemented on the process four proportional integral (PI) controllers with the following parameters for proportional gain $K_{ci} = 0.65$ and integral time constant $\tau_{Ii} = 10.0$ for $i = 1,2,3,4$ (these values were computed through extensive trial and error). The ith PI controller is used to adjust the power of the ith concentric lamp by using a point temperature measurement at $r = (i-1)/3$. The spatiotemporal evolution of the wafer temperature (top plot), the temperature distribution along the radius of the wafer at $t = 40\,\mathrm{s}$ (middle plot), and the thickness of the deposition (bottom plot–dashed line) are displayed in figure 7, and the corresponding manipulated input profiles are shown in figure 8. The performance of the four proportional integral controllers is significantly inferior (more than 5% variation in final thin film thickness) to the one obtained by the non-linear output feedback controller (see comparison in bottom plot of figure 7).
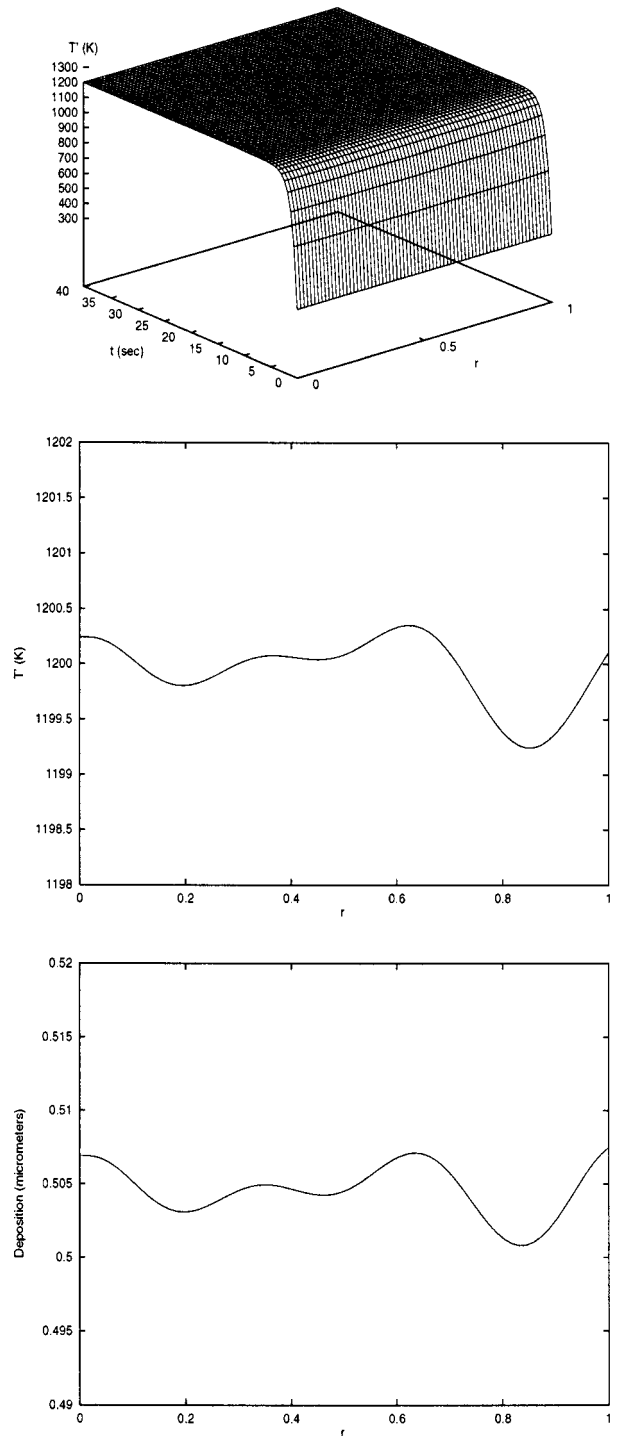

Figure 5. Closed-loop spatiotemporal wafer temperature profile (top figure), wafer temperature profile at $t = 40\,\mathrm{s}$ (middle figure), and deposition thickness profile at $t = 40\,\mathrm{s}$ (bottom figure) under non-linear control.

Remark 10: We finally note that the fifth-order model which was used for the design of the non-linear output feedback controllers in the above RTCVD process was obtained by using standard Galerkin's method and no improvement of its accuracy was pursued by using ap-
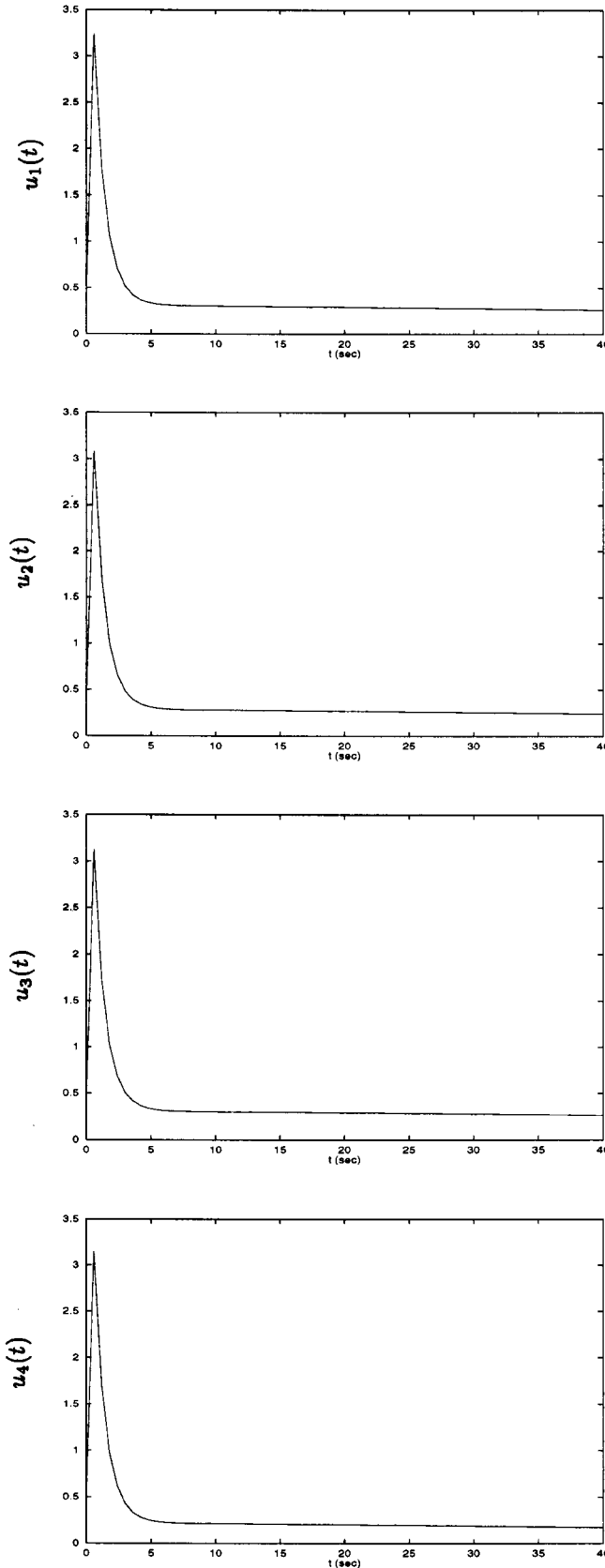
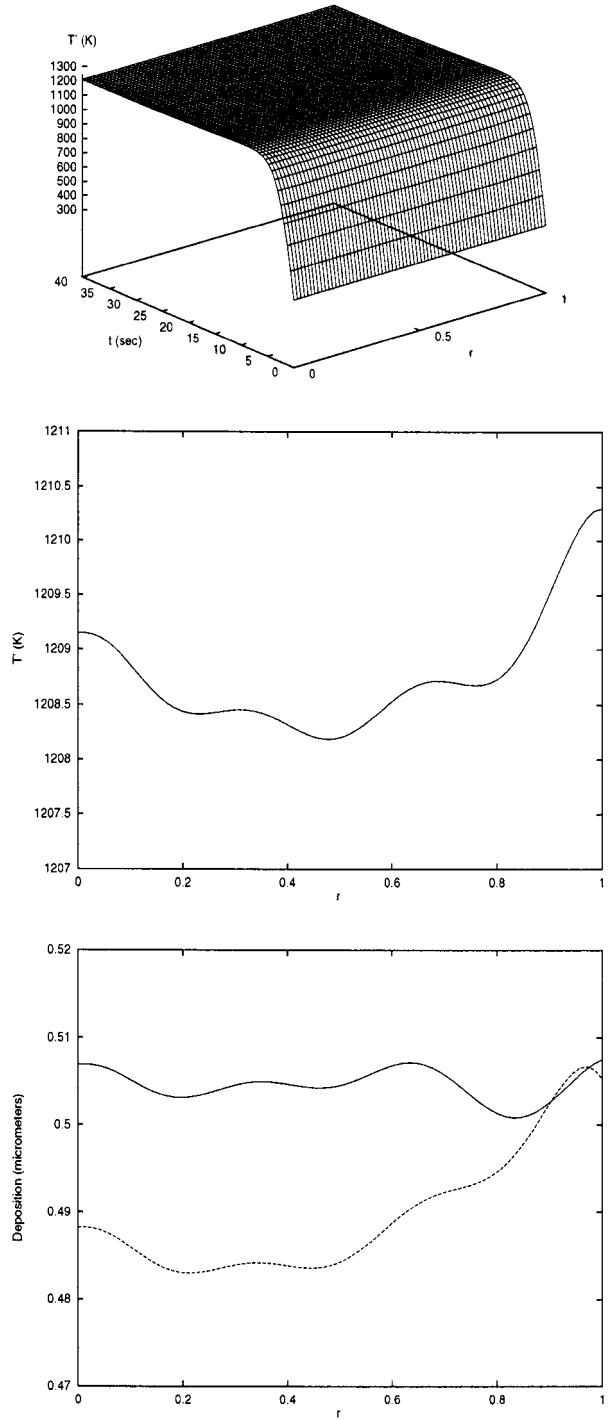Figure 6. Manipulated input profiles under non-linear control.

Figure 7. Closed-loop spatiotemporal wafer temperature profile (top figure) and wafer temperature profile at $t = 40\,\mathrm{s}$ (middle figure) under proportional integral control. Deposition thickness profiles at $t = 40\,\mathrm{s}$ (bottom figure) under proportional integral control (dashed line) and non-linear control (solid line).

proximate inertial manifolds. The reason is that the closed-loop performance of the non-linear controllers, synthesized by using this model, is clearly excellent (see the closed-loop deposition rate and temperature
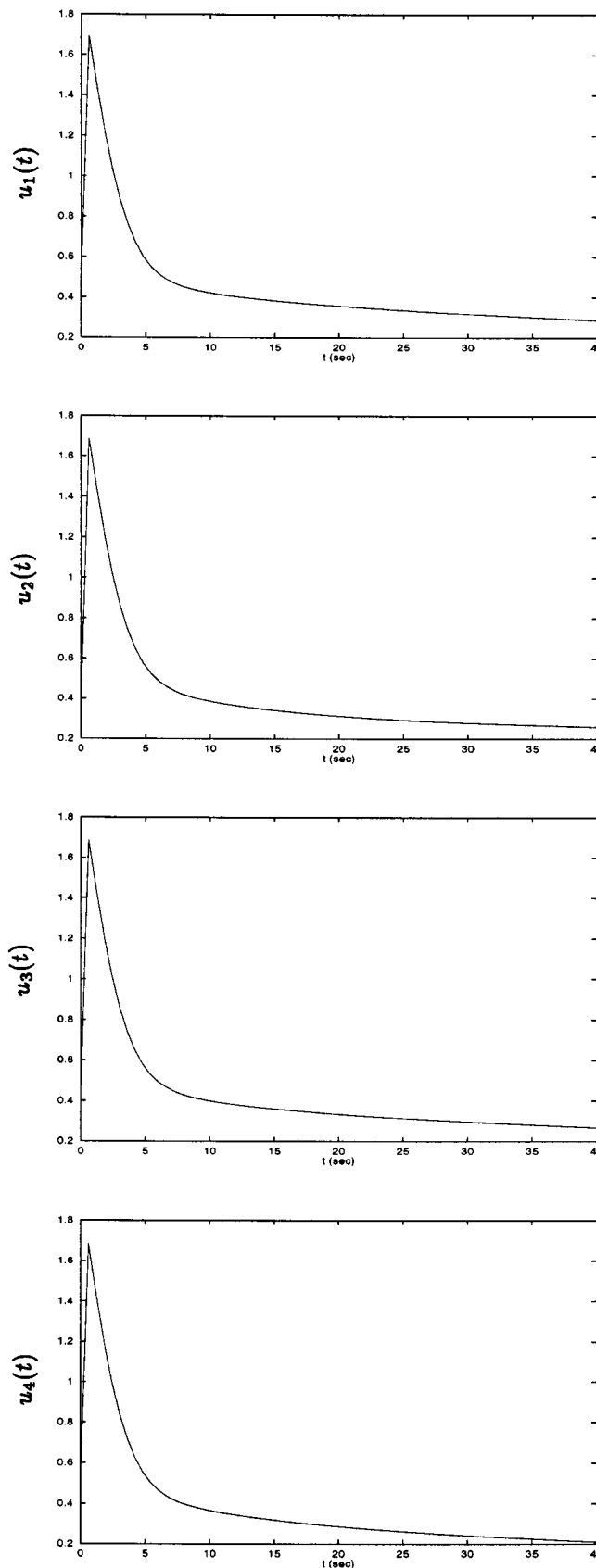
Figure 8. Manipulated input profiles under proportional integral control.

profiles in figure 5), thereby leaving no room for further improvement of the performance of the controller by using approximate inertial manifolds.

7. Conclusions

This article presented a general and practical method for the derivation of accurate finite-dimensional approximations and the synthesis of non-linear output feedback controllers for non-linear parabolic PDE systems for which the manipulated inputs, the controlled and measured outputs are distributed in space. The method involves three steps: first, the Karhunen–Loéve expansion is used to derive empirical eigenfunctions of the non-linear parabolic PDE system, then the empirical eigenfunctions are used as basis functions within a Galerkin's and approximate inertial manifold model reduction framework to derive low-order ODE systems that accurately describe the dominant dynamics of the PDE system, and finally, these ODE systems are used for the synthesis of non-linear dynamic output feedback controllers that guarantee stability and enforce output tracking in the closed-loop system. The proposed method was successfully applied to an RTCVD process and was shown to outperform conventional control schemes.

Acknowledgment

References

BANERJEE, S., COLE, J. V., and JENSEN, K. F., 1998, Nonlinear model reduction of rapid thermal processing systems. *IEEE Transactions on Semiconductor Manufacturing*, **11**, 266–275.

BANGIA, A. K., BATCHO, P. F., KEVREKIDIS, I. G., and KARNIADAKIS, G. E., 1997, Unsteady 2-D flows in complex geometries: comparative bifurcation studies with global eigenfunction expansion. *SIAM Journal on Scientific Computing*, **18**, 775–805.

BALAS, M. J., 1979, Feedback control of linear diffusion processes. *International Journal of Control*, **29**, 523–533.

BALAS, M. J., 1991, Nonlinear finite-dimensional control of a class of nonlinear distributed parameter systems using residual mode filters: a proof of local exponential stability. *Journal of Mathematical Analysis and Applications*, **162**, 63–70.

BREEDIJK, T., EDGAR, T. F., and TRACHTENBERG, I., 1993, A model predictive controller for multivariable temperature control in rapid thermal processing. *Proceedings of American Control Conference*, San Francisco, CA, USA, pp. 2980-2984.

CHEN, C. C., and CHANG, H. C., 1992, Accelerated disturbance damping of an unknown distributed system by nonlinear feedback. *AIChE Journal*, **38**, 1461–1476.

CHRISTOFIDES, P. D., 1998, Robust control of parabolic PDE systems. *Chem. Eng. Sci.*, **53**, 2949–2965.

CHRISTOFIDES, P. D., 2000, *Nonlinear and Robust Control of PDE Systems: Methods and Applications to Transport-Reaction Processes* (Boston: Birkhäuser), to appear.

CHRISTOFIDES, P. D., and DAOUTIDIS, P., 1996a, Nonlinear control of diffusion-convection-reaction processes. *Comp. Chem. Engng.*, **20(s)**, 1071–1076.

CHRISTOFIDES, P. D., and DAOUTIDIS, P., 1996b, Feedback control of hyperbolic PDE systems. *AIChE Journal,* **42**, 3063–3086.

CHRISTOFIDES, P. D., and DAOUTIDIS, P., 1997, Finite-dimensional control of parabolic PDE systems using approximate inertial manifolds. *Journal of Mathematical Analysis and Applications,* **216**, 398–420.

FOIAS, C., SELL, G.R., and TITI, E.S., 1989, Exponential tracking and approximation of inertial manifolds for dissipative equations. *Journal of Dynamics and Differential Equations,* **1**, 199–244.

FUKUNAGA, K., 1990, *Introduction to Statistical Pattern Recognition* (New York: Academic Press).

GRAHAM, M. D., and KEVREKIDIS, I. G., 1996, Alternative approaches to the Karhunen–Loéve decomposition for model reduction and rata analysis. *Comp. & Chem. Eng.*, **20**, 495–506.

HOLMES, P., LUMLEY, J. L., and BERKOOZ, G. 1996, *Turbulence, Coherent Structures, Dynamical Systems and Symmetry*, (New York: Cambridge University Press).

ISIDORI, A., 1989, *Nonlinear Control Systems: An Introduction* (Berlin: Springer-Verlag).

KIETHER, W. J., FORDHAM, M. J., YU, S., NETO, J. S., CONRAD, K. A., HAUSER, J. R., SORRELL, F. Y., and WORTMAN, J. J., 1994, Three-zone rapid thermal processor system. *Proceedings of 2nd International RTP Conference*, pp. 96–101.

KHALIL, H. K., 1992, *Nonlinear Systems* (New York: Macmillan Publishing Company).

KOKOTOVIC, P. V., KHALIL, H. K., and O'REILLY, J., 1986, *Singular Perturbations in Control: Analysis and Design* (London: Academic Press).

MARQUARDT, W., 1990, Traveling waves in chemical processes. *Int. Chem. Engng.*, **4**, 585–606.

PARK, H. M., and CHO, D. H., 1996, The use of the Karhunen–Loéve decomposition for the modeling of distributed parameter systems. *Chem. Eng. Sci.*, **51**, 81–98.

RAY, W. H., 1981, *Advanced Process Control* (New York: McGraw-Hill).

SHVARTSMAN, S. Y., and KEVREKIDIS, I. G., 1998, Nonlinear model reduction for control of distributed parameter systems: a computer assisted study. *AIChE Journal,* **44**, 1579–1595.

SIROVICH, L., 1987a, Turbulence and the dynamics of coherent structures: part I: coherent structures. *Quarterly of Applied Mathematics*, **XLV**, 561–571.

SIROVICH, L., 1987b, Turbulence and the dynamics of coherent structures: part II: symmetries and transformations. *Quarterly of Applied Mathematics*, **XLV**, 573–582.

TEMAM, R., 1988, *Infinite-Dimensional Dynamical Systems in Mechanics and Physics* (New York: Springer-Verlag).

THEODOROPOULOU, A., ADOMAITIS, R. A., and ZAFIRIOU, E., 1998, Model reduction for optimization of rapid thermal chemical vapor deposition systems. *IEEE Transactions on Semiconductor Manufacturing,* **11**, 85–98.

THEODOROPOULOU, A., ADOMAITIS, R. A., and ZAFIRIOU, E., 1999, Inverse model based real-time control for temperature uniformity of RTCVD. *IEEE Transactions on Semiconductor Manufacturing,* **12**, 87–101.